HHS Public Access

Author manuscript

J Cell Physiol. Author manuscript; available in PMC 2019 October 01.

Published in final edited form as:

J Cell Physiol. 2018 October ; 233(10): 6877–6895. doi:10.1002/jcp.26578.

Tctex-1, a novel interaction partner of Kidney Injury Molecule-1, is required for efferocytosis

Ola Z. Ismail[1], **Saranga Sriranganathan**[1], **Xizhong Zhang**[1], **Joseph V. Bonventre**[2], **Antonis S. Zervos**[3], and **Lakshman Gunaratnam**[1,4]

[1]Matthew Mailing Center for Translational Transplant Studies, London Health Sciences Center, Lawson Health Research Institute, London, Ontario, Canada

[2]Renal Division, Department of Medicine, Brigham and Women's Hospital, Harvard Medical School, Boston, Massachusetts

[3]Burnett School of Biomedical Sciences, University of Central Florida College of Medicine, Orlando, Florida

[4]Division of Nephrology, Department of Medicine, Schulich School of Medicine and Dentistry, London, Western University, Ontario, Canada

Abstract

Kidney injury molecule-1 (KIM-1) is a phosphatidylserine receptor that is specifically upregulated on proximal tubular epithelial cells (PTECs) during acute kidney injury and mitigates tissue damage by mediating efferocytosis (the phagocytic clearance of apoptotic cells). The signaling molecules that regulate efferocytosis in TECs are not well understood. Using a yeast two-hybrid screen, we identified the dynein light chain protein, Tctex-1, as a novel KIM-1-interacting protein. Immunoprecipitation and confocal imaging studies suggested that Tctex-1 associates with KIM-1 in cells at baseline, but, dissociates from KIM-1 within 90 min of initiation of efferocytosis. Interfering with actin or microtubule polymerization interestingly prevented the dissociation of KIM-1 from Tctex-1. Moreover, the subcellular localization of Tctex-1 changed from being microtubule-associated to mainly cytosolic upon expression of KIM-1. Short hairpin RNA-mediated silencing of endogenous Tctex-1 in cells significantly inhibited efferocytosis to levels comparable to that of knock down of KIM-1 in the same cells. Importantly, Tctex-1 was not involved in the delivery of KIM-1 to the cell-surface. On the other hand, KIM-1 expression significantly inhibited the phosphorylation of Tctex-1 at threonine 94 (T94), a post-translational

Correspondence: Dr. Lakshman Gunaratnam, Division of Nephrology, Department of Medicine, Schulich School of Medicine and Dentistry, London, Western University, 339 Windermere Road, Room A10-208, London, Ontario N6A 5A5, Canada. lakshman.Gunaratnam@lhsc.on.ca.

AUTHORS' CONTRIBUTIONS

O.I. made substantial contributions to data collection, analysis and manuscript preparation. S.S. contributed to analysis and editing the manuscript. S.S. and X.Z. contributed to data collection. J.V.B. provided essential reagents. J.V.B. and A.S.Z. contributed to interpretation of some of the data. The yeast two-hybrid screen and analysis were performed in A.S.Z. laboratory. A.S.Z. and S.S. edited the manuscript. L.G. made substantial contributions to the conception, design of the work, data analysis, interpretation of data, editing the manuscript, and was responsible for approving the final version of the manuscript.

CONFLICTS OF INTEREST

The authors declare that they have no conflicts of interest with the contents of this article.

SUPPORTING INFORMATION

Additional Supporting Information may be found online in the supporting information tab for this article.

modification which is known to disrupt the binding of Tctex-1 to dynein on microtubules. In keeping with this, we found that KIM-1 bound less efficiently to the phosphomimic (T94E) mutant of Tctex-1 compared to wild type Tctex-1. Surprisingly, expression of Tctex-1 T94E did not influence KIM-1-mediated efferocytosis. Our studies uncover a previously unknown role for Tctex-1 in KIM-1-dependent efferocytosis in epithelial cells.

Keywords

cytoskeleton; efferocytosis; kidney injury molecule-1; phagocytosis; tctex-1

INTRODUCTION

The process of programmed cell death, or apoptosis, is characterized by distinct morphological characteristics that serve as a mechanism for removing damaged or unwanted cells from the organism (Kerr, 2002; Kerr, Wyllie, & Currie, 1972; Wyllie, Kerr, & Currie, 1980). Phagocytosis of apoptotic cells, termed efferocytosis (Vandivier, Henson, & Douglas, 2006), prevents the release of noxious and immunogenic materials from dying cells, which reduces inflammation or inappropriate autoimmune response (Ren & Savill, 1998). Efferocytosis is increasingly recognized to be important in tissue repair as well, for instance after acute organ injury (Juncadella et al., 2013). Efferocytosis is usually carried out by professional phagocytes (Albert et al., 1998; Duvall, Wyllie, & Morris, 1985), however, amateur phagocytes, such as fibroblasts, retinal pigment epithelial cells, sertoli cells, and more recently renal proximal tubular epithelial cells, also play roles in this process (Finnemann, Bonilha, Marmorstein, & Rodriguez-Boulan, 1997; Ichimura et al., 2008; Monks, Geske, Lehman, & Fadok, 2002; Patel et al., 2010; Shiratsuchi, Umeda, Ohba, & Nakanishi, 1997). The direct or indirect recognition of apoptotic cells by phagocytes involves the recognition of “eat-me” signals that are newly (e.g., exposed or modified lipids or proteins) exposed on the surface of apoptotic cells. One of the most well characterized of these signals is phosphatidylserine (PS) (Ravichandran & Lorenz, 2007).

Kidney injury molecule-1 (KIM-1) is a well characterized efferocytosis receptor that is expressed on injured renal proximal tubular epithelial cells (TECs) (Ichimura et al., 1998, 2008). It recognizes phosphatidylserine on the surface of apoptotic cells (Ichimura et al., 2008; Kobayashi et al., 2007; Miyanishi et al., 2007). KIM-1 was first identified in a cDNA screen looking for proteins localized to the apical membrane of TECs following injury to kidney commonly caused by ischemia or toxic insult (Ichimura et al., 1998). KIM-1 is a type I transmembrane glycoprotein consisting of an N-terminal immunoglobulin V (IgV) domain, a mucin domain, a transmembrane domain, and a cytoplasmic tail (Ichimura et al., 1998; Santiago et al., 2007). The signaling mechanism and downstream mediators of phagocytic signaling underlying KIM-1-mediated uptake of apoptotic cells are only now beginning to be identified. Previously, KIM-1 was shown to interact with p85 following apoptotic cell binding (Yang et al., 2015). This was shown to lead to down-regulation of the NF-κB pathway and subsequent inhibition of inflammatory signaling during AKI. In addition, we uncovered that KIM-1 interacts with the a subunit of heterotrimeric G12 protein (Gα12) and inhibits its activity to enable efficient efferocytosis (Ismail et al., 2015; Ismail, Zhang,

Bonventre, & Gunaratnam, 2016). KIM-1-inhibition of Gα12-dependent RhoA activity was specifically key for enabling KIM-1-mediated efferocytosis as RhoA inhibits this process (Ismail et al., 2016; Nakaya, Tanaka, Okabe, Hanayama, & Nagata, 2006). Though several proteins have been identified to interact with KIM-1, the detailed signaling mechanisms by which KIM-1 regulates the uptake of apoptotic cells has not yet been fully elucidated.

Here we used a yeast two-hybrid system to screen a HeLa cDNA library to identify potential interactors of the cytoplasmic tail of KIM-1 (aa 311–359). In this screen, Tctex-1 (or t-Complex testis-expressed-1 or Dynein light chain Tctex-type 1 [DYNLT1 for short, hereon is referred to as Tctex-1]) (King, Benashski, Lye, Patel-King, & Pfister, 1996; Lader, Ha, O'Neill, Artzt, & Bennett, 1989) was isolated as a specific interactor of the LexA-KIM-$1_{311–359}$ bait. Tctex-1 (Dynein Light Chain Tctex-Type 1 protein coding gene) was previously identified in a screen looking for candidate genes of the mouse t complex whose aberrant expression may be functionally related to sterility and transmission ratio distortion (Lader et al., 1989). It is a key component of the cytoplasmic light chain of the dynein motor complex (King et al., 1996). Cytoplasmic dynein is a multicomponent, microtubule-based, ATP-dependent motor unit that has several roles in intracellular retrograde transport, mitotic spindle localization, and centrosome separation (Barton and Goldstein, 1996; Schroer, 1994; Steuer, Wordeman, Schroer, & Sheetz, 1990). Tctex-1 plays diverse dynein-dependent and -independent functions (Hirokawa, 1998; Hirokawa, Noda, & Okada, 1998; Lader et al., 1989). Through dynein-dependent functions, Tctex-1 is associated with microtubules in order to mediate a range of intracellular motile events that are important in the intracellular targeting or sorting of proteins (Mueller, Cao, Welker, & Wimmer, 2002; Sachdev et al., 2007; Tai, Chuang, Bode, Wolfrum, & Sung, 1999;). For example, Tctex-1 interacts with rhodopsin, a GPCR, and transports vesicles containing rhodopsin from the Golgi apparatus to the apical cell surface via tethering of Tctex-1 to the dynein complex on microtubules (Tai et al., 1999; Tai, Chuang, & Sung, 2001). On the other hand, Tctex-1 has been shown to function independent of dynein, to regulate actin cytoskeletal dynamics (Chuang et al., 2005). Phosphorylation of Tctex-1 at Threonine-94 (Thr-94) has been shown to promote its dissociation from the dynein light chain and may allow it to bind to other non-dynein proteins to mediate dynein-independent functions (Chuang et al., 2005; Song, Benison, Nyarko, Hays, & Barbar, 2007). In addition, Tctex-1 expression is restricted to certain tissues, where immunoprecipitation of kidney, spleen, and testis tissues lysate showed higher levels of Tctex-1 than brain tissue lysate (King et al., 1996). Despite advances in the research regarding Tctex-1, most of the research into this protein has focused on the role of Tctex-1 in neurogenesis, with little information about its role in the kidney (Tai et al., 2001).

In this report, in addition to uncovering the novel interaction between Tctex-1 and KIM-1, we demonstrate a key role for this protein in efferocytosis for the first time. We showed that Tctex-1 is phosphorylated upon stimulation of KIM-1-expressing cells with apoptotic cells in a manner that is KIM-1-dependent. A phosphomimetic mutant of Tctex-1 (dynein-independent form) interacted less efficiently with KIM-1 compared to wild type Tctex-1 or phosphorylation-defective mutant of Tctex-1. Finally, we provide evidence to suggest that Tctex-1 likely modulates KIM-1-dependent efferocytosis independent of the delivery of KIM-1 to the apical surface of cells (Yeh, Peretti, Chuang, Rodriguez-Boulan, & Sung,

2006). Altogether, our findings support the idea that Tctex-1 is an important signaling protein downstream of KIM-1 that is required for efferocytosis.

MATERIALS AND METHODS

Cell culture and materials

Human Embryonic Kidney 293 (HEK-293) cells and human renal adenocarcinoma cell lines (769-P) were cultured at 37 °C in 5% (vol/vol) CO_2 incubator and maintained in DMEM or RPMI media (Invitrogen, Carlsbad, CA) containing 10% FBS (Invitrogen). Chemicals were purchased from Sigma (Sigma-Aldrich, St. Louis, MO) unless stated. The pH-sensitive dye pHrodo™ Red succinimidyl ester (pHrodo™ Red, SE), Alexa Fluor® 555 goat anti-mouse, Alexa Fluor® 488 goat anti-mouse, Alexa Fluor® 488 goat anti-rabbit and DAPI (4′,6-diamidino-2-phenylindole) were purchased from Life Technologies (Molecular probes, Invitrogen). Cy3 conjugated-anti-tubulin antibody (ab.Tub2.1) was purchased from Abcam (Cambridge, MA). Flag-tag or (DYKDDDDK Tag) Antibody (#5407) conjugated with Alexa Fluor® 488 Conjugate was purchased from Cell Signaling Technology (Cell Signaling Technology, Danvers, MA). Rhodamine phalloidin stain was purchased from Cytoskeleton Inc., (Denver, CO). DYNLT-1 antibody used for confocal microscopy was purchased from Proteintech Group Inc., (Chicago, IL) (1:50). Antibodies for Western blot against Tctex-1 (1:800), actin (1:1000) were all purchased from Sigma-Aldrich. PE-conjugated anti-human KIM-1 (1:100, clone 1D12) and PE-conjugated rat lgG2b isotype control (1:100, clone RTK4530) were purchased from Biolegend (San Diego, CA). Anti-KIM-1 (cytosolic domain) antibody was generated by immunizing rabbits against the cytosolic domain of KIM-1 (Life Technologies, custom made) as previously described (Bailly et al., 2002; Tai et al., 1999). KIM-1 antibody binding to the mucin domain of KIM-1 (AKG7) was kindly provided by Dr. Bonventure (Harvard Medical School, Brigham, and Women's Hospital, Boston, MA). The anti-Phosphothreonine antibody (ab9337) was purchased from Abcam. Complete Mini EDTA-free protease inhibitor cocktail tablets were purchased from Roche Diagnostic (Basel, Switzerland). Cytochalasin D and Nocodazole were purchased from EMD Millipore (Billerica, MA). Plasmid constructs for DYNLTl/Tctex-1 were kindly provided by Dr. Robert Rottapel (University of Toronto, Toronto, ON) and plasmid constructs for KIM-1 were from Dr. Bonventre (Harvard Medical School, Brigham, and Women's Hospital). Lipofectamine® 2000 (Life Technologies, Thermo Fisher Scientific, Rockford, IL) was used for transfecting plasmid.

Yeast two-hybrid screening of KIM-1 interactors

The following primers were used to PCR a DNA fragment corresponding to the unique cytoplasmic domain of human KIM-1 (aa 311–359): KIM-1 Fw 5′ ATAGCTGAATTCAAAAAGTATTTCTTCAAAAAGGAGGTTCAACAA-3″, Rw 5′ TAGCTCTCGAGTTAGTCCGTGGCATAAAGACTATT-3′. Primers were designed with an EcoRI site at the 5′ end and an Xho1 site at the 3′ end. PCR products were digested and cloned in frame into the prey pJG4–5 vector as previously described (Cilenti et al., JBC 279 (2004) 50295–50301). The EGY 48 yeast strain was transfected with pGilda-KIM-$1_{311–359}$ and the expression and stability of the bait was monitored using Western blot analysis and LexA antibodies (Ambivero, Cilenti, Main, & Zervos, 2014). A HeLa cDNA library was

screened and several interactors were isolated. These interactors were characterized by DNA sequencing and their specificity against the LexA-KIM-$1_{311–359}$ was further tested as described (Ambivero et al., 2014; Zervos, Gyuris, & Brent, 1993).

Immunoprecipitation and Western blot

Cells were lysed with ice-cold lysis buffer containing 50 mM Tris-HCI, pH 7.5, 150 mM NaCI, 2 mM EDTA, 1 mM $NaVO_4$, 1 mM NaF, 1% Triton X-100, and complete mini EDTA-free protease inhibitor cocktail tablets (Roche Diagnostic). For immunoprecipitation, cell extracts containing 1.0–1.5 mg of the protein/ml were incubated with 10 μg of KIM-1 (cytosolic domain), or rabbit IgG (control) antibody and 20 μl of protein-A/G Sepharose beads (Santa Cruz Biotechnology, Santa Cruz, CA) at 4 °C overnight. Beads were centrifuged, washed three times, and suspended in 20 μL of SDS sample buffer and heated at 100 °C for 5 min. Lysates (representing 5% of total lysate) and immunoprecipitation samples were separated under reducing condition and transferred to polyvinylidene difluroide (PDVF) membranes (EMD Millipore). PDVF-membranes were probed with antibodies specific to mucin domain of KIM-1 (AKG7) (1:1 dilution), cytosolic domain of KIM-1 (1:1,500 dilution), Tctex-1 (1:800 dilution) or actin (1:2,000 dilution). The signal was visualized using the appropriate horseradish peroxidase-conjugated secondary antibodies and ECL western blot detection reagent (Luminata forte, EMD Millipore) and by autoradiography (Biomax; Denville Scientific, South Plainfield, NJ).

GST-Tctex-1 pull down

The GST- Tctex-1 construct was transformed into *E. coli* strain BL21 and expression of the fusion protein was induced by addition of 0.3 mM isopropyl-β-D-thiogalactopyranoside (IPTG) for 3 hr at 37 °C. After lysing the bacterial cells by sonication, GST-fusion proteins were purified by incubation with 1 ml of glutathione-Sepharose beads (Thermo Fisher Scientific) overnight at 4 °C. This was followed by three washes with 1× PBS and aliqoutes of GST-Tctex-1 conjugated to glutathione-Sepharose beads were kept at −80 °C for future use. Cells were lysed with ice-cold lysis buffer(50 mM Tris-HCI, pH 7.5,150 mM NaCI, 2 mM EDTA, 1mM $NaVO_4$, 1 mM NaF, 1% Triton X-100) supplemented with complete mini EDTA-free protease inhibitor cocktail tablets (Roche Diagnostic). 1 mg of protein lysate and 30ul of GST-Tctex-1 coupled glutathione-Sepharose beads were incubated together at 4 °C for overnight. Beads were washed to remove non-specific binding and eluted using 20 μL of SDS sample buffer and heated at 100 °C for 5 min. Both lysate and pull-down samples were analyzed by SDS-PAGE and Western blotting to represent total and pull-down results, respectively.

Immunofluorescence and confocal microscopy

HEK-293 cells were cultured at subconfluent density on poly-D-lysine hydrobromide (Sigma-Aldrich) coated glass cover slips, and were transfected with constructs encoding KIM-1 and flag-tagged Tctex-1. 769-P cells were grown on glass cover slips (without coating) and fed fluorescently labelled apoptotic cells with pH-sensitive dye pHrodo™ Red succinimidyl ester (Life Technologies, Molecular probes, Invitrogen) for indicated time points (15–90 minutes). Cells were washed three times with 1× PBS. Cells were fixed with 4% paraformaldehyde followed by counterstaining of the nucleus with DAPI (0.5 μg/ml).

Cells were then permeabilized with 0.25% Triton X–100 in 1× PBS for 5 min, and then blocked for 1 hr at room temperature with 1% Bovine serum albumin (BSA) and 0.05% Triton X–100 in 1× PBS. Cells were then incubated with Tctex-1(1:50) (Proteintech Group Inc.) in 0.5% BSA/PBS at 4 °C overnight. Coverslips were washed three times with PBS and incubated with Alexa Fluor® 488 goat anti-rabbit (1:500) at 37 °C for 1 hr. For flag-tag staining, cells were incubated with flag-tag antibody conjugated with Alexa Fluor 488 (1:400) overnight. For surface staining of KIM-1, coverslips were washed three times with PBS and incubated with antibody against mucin domain of KIM-1 (AKG) (1:1) at 4°C overnight. Bound KIM-1 was labelled with Alexa 555 conjugated antimouse (1:1,000) at room temperature for 1 hr. The specificity of immunostaining was demonstrated by the absence of signal in sample processed using non-specific rabbit or mouse IgG followed by staining with the proper secondary antibody. For cytoskeleton staining, cells were permeabilized with 0.25% Triton in 1× PBS for 5 min, and then stained with overnight with Cy3-conjugated anti-tubulin antibody (Abcam). Coverslips were mounted using Shandon-Mount® permanent mounting (Thermo Fisher Scientific) and viewed with FLUOVIEW X83I confocal microscopy (Olympus, Tokyo, Japan). Data were acquired and analyzed using FLUOVIEW FV10 ASW 4.0 viewer and ImageJ software (National Institutes of Health, Bethesda, MD) to determine Pearson's coefficient and Van Steensel score for colocalization of KIM-1 and Tctex-1. Quantification of number of colocalization score was assessed in three random fields per sample and was done in three independent experiments.

Phagocytosis assay and FACS analysis

To prepare apoptotic cells for phagocytosis assay, thymocytes were harvested from 3 to 6 weeks old C57BL/6 mice, and apoptosis was induced by UV exposure for 5 min followed by incubation overnight at 37 °C in 5% CO_2 incubator in DMEM media supplemented by 10% FBS and 1% Penicillin-streptomycin solution. Apoptotic thymocytes were stained with pH-sensitive dye pHrodo™ Red succinimidyl ester (pHrodo™ Red, SE) at final concentration of 150nM for 30 min at room temperature. Labelled apoptotic cells were washed twice with 1× PBS to remove access dye. The cells were counted and 3×10^6 were added to each well of six-well plate (15×10^6 for 10 cm plates) and incubated for various time points at 37 °C in 5% CO_2 incubator. Cells were then placed on ice for 30 min to reduce non-specific binding of apoptotic cells. The plates were then washed three times with ice-cold 1× PBS, and cells were collected with 5 mM EDTA-PBS, and resuspended with FACS buffer (1×Phosphate-buffered saline [PBS], 2% calf serum, and 0.1% sodium azide) for flow analysis. For KIM-1-surface staining, the cells were blocked in PBS and 10% goat serum for 15 min, followed by incubation for 30 min at room temperature with PE-conjugated anti-KIM-1 (human) and respective isotype control antibody at concentration of 1:100. All samples were run on BD LSR II flow cytometer (BD Biosciences, San Jose, CA). Percentage of phagocytosis represented the number of cells that have internalized the apoptotic cell(s) as indicated by higher fluorescence (10^4–10^5 on logarithmic scale). The ratio of phagocytosis was calculated by dividing the percentage of uptake of apoptotic cells in treated cells or transfected cells by the percentage of uptake of apoptotic cells in vehicle treated cells or cells transfected with control plasmid. Engulfed cells with low fluorescence were excluded from analysis.

ShRNA Tctex-1

shRNA Lentiviral Particles containing control shRNA, Tctex-1 shRNA, and KIM-1 shRNA were purchased from Santa Cruz Biotechnology. Cells were transfected according to manufacturer suggestion. Transfected cells were kept underselection using 2 μg/ml puromycin dihydrochloride (Santa Cruz Biotechnology) for 2 weeks prior to confirm a successful knockdown using Western blotting and FACS.

QPCR

KIM-1, Tctex-1, and GAPDH level was measured with quantitative PCR. The RNA was extracted from cells using TRIzol™ Reagent (Ambion®, Thermo Fisher Scientific, Waltham, MA) in accordance with the manufacturer's instructions. The quality of RNA was verified by measuring the samples absorbencies at 260 and 280 nm. The RNA was reversely transcribed into cDNA using qScript™ cDNA SuperMix (QuantaBio, Beverly, MA). qPCR was performed using SYBR selected master mix (Life Technology, Thermo Fisher Scientific, Waltham, MA) and StepOne System (Applied biosystem, Thermo Fisher Scientific, Waltham, MA). Melt curve was performed at the end of each reaction to verify PCR product specificity. The results were normalized to GAPDH expression measured in each sample. Primers were designed and ordered via IDT-Integrated DNA technologies (IDT Inc., Coralville, IA). Primer sequences for Tctex-1: F: 5′-CTGCGGAGGAGACTGCTTTT-3′; R: 5′ AGCAGGAACT TGCTGTGTGT-3′. KIM-1: F: 5′-CTG CCT ATC ACAACG CAG AA-3′; R: 5′-TTCTTC CAG CAC CAC AGA AG-3′. GAPDH: F: 5′-GGATTTGGTCGTATTGGG-3′; R: 5′-GGAA GATGGTGATGGGATT-3′.

Rac1 and RhoA activation

Rac1 or RhoA activation was determined using G-LISA Rac1 or RhoA activity assay according to the manufacturer's instructions (Cytoskeleton, Denver, CO). Total RhoA was determined using Total RhoA ELISA kit (Cytoskeleton). A total of 40 μg of protein was used for activation assay and 20 μg of protein was used for total RhoA assay. Treatment with 5% serum after serum starvation overnight served as positive control for Rac1 activation (Curtiss et al., 2011). Treatment of cells with 10 μM Nocodazole for 15 min served as positive control for RhoA activation as indicated previously (Yano, Cong, Birge, Goff, & Chao, 2000).

Quantification and statistics

Western blots were scanned and band intensity quantified using ImageJ software (National Institutes of Health) after subtracting background and determining linear range. Level of interaction of two proteins was determined by dividing the intensity value (obtained from Western blotting) of protein being co-immunoprecipitated (Tctex-1) by the intensity value of protein being immunoprecipitated (KIM-1). Graphs were obtained by using GraphPad Prism software (Graph Pad Software, Inc., La Jolla, CA). Statistics were done using IBM SPSS statistic 22 (IBM, Armonk, NY). Significance was determined by using one-way ANOVA with Tukey post hoc test or unpaired t test where indicated.

RESULTS

KIM-1 interacts with Tctex-1 during the early phase of efferocytosis

The cytosolic domain of KIM-1 (amino acids 311–359) has been shown to mediate cell signaling in a variety of cell types including T cells (Binne, Scott, & Rennert, 2007; Curtiss et al., 2011) and kidney TECs (Balasubramanian, Kota, Kuchroo, Humphreys, & Strom, 2012; Ismail et al., 2015; Yang et al., 2015). Though we previously uncovered a role for the heterotrimeric G-protein, Gα12/GNA12 in the negative regulation of efferocytosis (Ismail et al., 2015), to date the phagocytic signaling pathway(s) that regulate KIM-1-dependent efferocytosis remains largely unknown. To this end, we performed a yeast-two-hybrid screen using the cytoplasmic tail of human KIM-1 $_{311–359}$ as a bait and screened a HeLa cDNA library to identify potential interacting proteins (Park et al., 2007; Zervos et al., 1993). Twelve interactors were isolated representing two different cDNAs: (a) Tctex-1/DYNTL1 (Lader et al., 1989); and (2) γ-aminobutyric acid type A receptor (Wang, Bedford, Brandon, Moss, & Olsen, 1999) (GABARAP) . Analysis of the interaction between Tctex-1 and KIM-1 $_{311–359}$ is shown in Supplementary Figure S1. Because of the important role that Tctex-1 plays in modulating actin cytoskeletal dynamics (Chuang et al., 2005; Meiri et al., 2012), and the requirement of the cytoskeleton for the formation of phagocytic arms during phagocytosis (Chimini & Chavrier, 2000), we selected the Tctex-1 for further study. To validate the results from the yeast two-hybrid screen, we performed co-immunoprecipitation (co-IP) experiments using HEK-293 cells that were transfected with both human GFP-tagged KIM-1 and human flag-tagged Tctex-1 (Figure 1a, Supplementary Figure S2). We further confirmed this interaction by detecting the colocalization of both proteins when overexpressed by HEK-293 cells via immunofluorescent labelling and confocal microscopy (Figure 1b).

Given the important role of KIM-1 (a phosphatidyserine receptor) in efferocytosis in the kidney (Ichimura et al., 2008; Kobayashi et al., 2007; Miyanishi et al., 2007), we sought to determine whether the interaction between KIM-1 and Tctex-1 remains intact during the course of phagocytosis. Using co-IP experiments, we found a significant decrease in the interaction between KIM-1 and Tctex-1 between 60 and 90 min (later stages of phagocytosis) after stimulation with apoptotic cells (Figure 1c). Though the exogenous expression of both proteins in HEK-293 cells provided evidence of the interaction, it did not necessarily reflect normal cellular physiology. To address this, we utilized the human renal adenocarcinoma cell line, 769-P, which endogenously expresses both human KIM-1 (Bailly et al., 2002) and Tctex-1 (Gunaratnam, unpublished data). Co-IP results obtained from 769-P cells confirmed the previously observed loss of interaction between KIM-1 and Tctex-1 during the later stages of phagocytosis (Figures 1d and 1e).

To further corroborate these data, GST pull-down assays were performed. A fusion protein consisting of GST fused to full-length Tctex-1 (GST- Tctex-1) was used to test GST- Tctex-1 interaction with KIM-1 during the course of phagocytosis (Gauthier-Fisher et al., 2009). As observed before, a significant reduction in the interaction between KIM-1 and GST- Tctex-1 was observed during the later stages of uptake of apoptotic cells (90 min) (Figures 1f and

1g). Taken together, these data confirmed that the interaction between KIM-1 and Tctex-1 is dynamic and appears to decline during the course of KIM-1-dependent phagocytosis.

Intracellular colocalization of Tctex-1 and KIM-1 occurs during the early stages of phagocytosis

We performed confocal immunofluorescence analysis to determine the degree of colocalization between KIM-1 and Tctex-1 during the course of apoptotic cell engulfment. Using an antibody directed against the extracellular domain of KIM-1 to stain for endogenous KIM-1 expression in 769-P cells, we found KIM-1 to be distributed on the cell-surface and within the intracellular compartments reminiscent of the golgi apparatus as previously reported (Machacek et al., 2009). On the other hand, immunostaining for endogenous Tctex-1 revealed diffuse cytoplasmic staining with some staining concentrated in the perinuclear region as previously reported (Campbell, Cooper, Dessing, Yates, & Buder, 1998). Double staining showed that both Tctex-1 and KIM-1 colocalized to the cytoplasmic compartment of the cells at baseline (prior to addition apoptotic cells) (Figure 2a). However, the colocalization of KIM-1 and Tctex-1 became decreased between 15 and 90 min of addition of apoptotic cells (Figure 2a). In order to quantify the colocalization images of KIM-1 and Tctex-1, we analyzed the results using JACoP software (as indicated in the experimental procedures section) to determine the Pearson's coefficient. We concluded that the level of colocalization decreased significantly during the later stages of phagocytosis (Figure 2b), consistent with the immunoprecipitation data presented above. Given the fact that some consider evaluating colocalization using Pearson's coefficient to be ambiguous as it incorporates noise and fluorescence intensity variation in analysis (Li et al., 2011), we also analyzed the data according to Van Steensel's approach (Wong, Pertz, Hahn, & Bourne, 2006). Similar to Pearson's coefficient, we found that the colocalization decreased significantly during later stages of apoptotic cells uptake (Figure 2c). These results suggest that during the process of KIM-1-mediated phagocytosis, there is a temporal decrease in the colocalization between KIM-1 and Tctex-1.

Interfering with actin or microtubule polymerization restores the interaction of KIM-1 with Tctex-1 during the later stages of phagocytosis

Previous results showed that the interaction between KIM-1 and Tctex-1 was influenced by events occurring during the late stages of phagocytosis. Local remodeling of the underlying actin cytoskeleton and microtubule network is crucial for corpse uptake during the later stages of efferocytosis (Freeman & Grinstein, 2014; Harrison & Grinstein, 2002; Toda, Hanayama, & Nagata, 2012). To determine the importance of actin and microtubule stability during KIM-1-mediated phagocytosis, we pretreated 769-P cells with cytochalasin D and nocodazole, inhibitors of actin filament polymerization and microtubule formation, respectively. The 769-P cells were subsequently fed fluorescently-labelled apoptotic cells and the level of uptake was determined by flow cytometry. As expected (Elliott et al., 2010; Hartwig, Davies, & Stossel, 1977), there was a significant reduction in the level of the uptake of apoptotic cells compared to the control-treated cells (Figure 3a). We then determine whether actin and microtubule changes that normally take place during phagocytosis contributed to the loss of KIM-1-Tctex-1 interaction. We performed co-IP following pretreatment with either vehicle, nocodazole or cytochalasin D, and stimulating

with apoptotic cells for 90 min. We observed a restoration of the interaction between KIM-1 and Tctex-1 following cytochalasin D and nocodazole treatment, to a level similar to unstimulated cells (Figures 3b and 3c). Altogether, these results suggest that disrupting the actin network or microtubule cytoskeleton strengthens the interaction between KIM-1 and Tctex-1. It is not clear if disruption of the KIM-1 and Tctex1 interaction is required for efferocytosis to proceed.

Tctex-1 mediates phagocytosis by KIM-1

The above data characterized the interaction between KIM-1 and Tctex-1 during phagocytosis, but did not identify whether Tctex-1 was required for phagocytosis of apoptotic cells. To test this, we transfected 769-P cells with lentiviral particles with either control shRNA (shControl), KIM-1 shRNA (shKIM-1), or Tctex-1 shRNA (shTctex-1) per manufacturer recommendation. We selected a heterogeneous population of the cells using puromycin dihydrochloride. The cells were lysed and protein level was determined using Western blotting (Figure 4a). The fold change in expression of KIM-1 and Tctex-1 in these cells was also determined using qPCR assay (Figure 4b). In order to test the sensitivity of Tctex-1 antibodies to its knockdown, the level of Tctex-1 expression in the cells was visualized using confocal microscopy (Figure 4c). These data confirmed that both Tctex-1 or KIM-1 were effectively knocked down in 769-P shTctex-1 or 769-P shKIM-1 cells, respectively. Next, these cells were fed fluorescently labelled apoptotic cells for 90 min and level of uptake was measured by flow cytometry. When we compared the phagocytic capacity between 769-P cells and 769-P cells with control shRNA to the Tctex-1 shRNA treated cells, Tctex-l-silenced cells exhibited a significant decrease in the level of uptake of apoptotic cells (Figure 4d). The degree to which efferocytosis was inhibited by shRNA against Tctex-1 was similar to that observed in 769-P with KIM-1 shRNA. As Tctex-1 had been shown to play a role in cellular cargo trafficking through its dynein-dependent function (Mueller et al., 2002; Palmer, MacCarthy-Morrogh, Smyllie, & Stephens, 2011; Tai et al., 1999), we determined whether silencing Tctex-1 inhibited phagocytosis because of decreased trafficking of KIM-1 to the cell-surface. To this end, we measured KIM-1 surface expression in 769-P cells with Tctex-1 shRNA and compared it to cells transfected with control shRNA or no shRNA (Figure 5a). We utilized 769-P with KIM-1 knockdown as a negative control in surface staining. We did not observe any significant difference in KIM-1 surface expression between 769-P, 769-P with control shRNA and 769-P cells with Tctex-1 shRNA (Figure 5b). Furthermore, we examined whether silencing Tctex-1 would affect cell viability by staining these different shRNA cells with PI (necrotic) or Annexin V (apoptotic) dye (Figure 5c). We failed to observe any significant difference between 769-P, 769-P shControl, 769-P shKIM-1, and 769-P shTctex-1 cells. The above data suggested that Tctex-1 plays an important positive role in KIM-1-mediated phagocytosis independent of affecting surface expression of KIM-1.

Threonine phosphorylation of endogenous Tctex-1 is enhanced following KIM-1 silencing

As Tctex-1 has been previously shown to associate with microtubules to mediate a range of intracellular motility events, such as retrograde trafficking in neurons and receptor trafficking (Sachdev et al., 2007; Tai, Chuang, & Sung, 1998), we assessed whether silencing KIM-1 expression would have an effect on Tctex-1 association with microtubules.

We, therefore, stained the KIM-1 knockdown and Tctex-1 knockdown cells with Cy3-conjugated beta-tubulin antibody and anti-Tctex-1 antibody to study the localization of Tctex-1 in the presence and absence of KIM-1 (Figure 6). Most of the KIM-1 silenced cells exhibited a highly organized tubulin-structure with Tctex-1 staining pattern that seemed to overlap with microtubule structures when compared to control shRNA cells. As the phosphorylation of Tctex-1 at Threonine-94 (Thr-94) has been shown to be a crucial step in the dissociation of Tctex-1 from the dynein light chain and consequently microtubule filaments (Chuang et al., 2005; Song et al., 2007), we tested whether Tctex-1 is phosphorylated in 769-P untransfected, or 769-P shControl and 769-P shKIM-1 cells. We performed immunoprecipitation of Tctex-1 followed by immunoblotting for Tctex-1 and phosphorylated threonine (pThr) in immunoprecipitated amount (Figure 7). We observed that Tctex-1 is not phosphorylated at baseline (and there is no difference) in shControl and shKIM-1 cells. However, when cells were stimulated with apoptotic cells, the level of Tctex-1 we observed increased phosphorylation of Tctex-1 in both shControl and shKIM-1 cells (Figure 7). Interestingly, the threonine phosphorylation was higher in shKIM-1 cells compared to the control cells when stimulated with apoptotic cells (Figure 7b). The above data suggest that KIM-1 suppresses the (Thr-94) phosphorylation of Tctex-1 that occurs following apoptotic cell-uptake.

Phosphomimetic mutant of Tctex-1 fails to interact with KIM-1, but does not affect KIM-1-mediated phagocytosis

Next, we sought to determine here whether the phosphorylation of Tctex-1 (and its ability to bind dynein) would influence its interaction with KIM-1. HEK-293 cells were transfected with KIM-1 and various Tctex-1 constructs. One of these plasmids expresses the phosphomimetic mutant of Tctex-1 (T94E), which fails to be incorporated into the dynein complex, resulting in a dynein-free form of Tctex-1 (Chuang et al., 2005). As a control, a construct encoding an unphosphorylated mimic of Tctex-1 mutant (T94A) was also used, As it has been shown to have a similar action to wild type Tctex-1 in its ability to bind to dynein complex (opposite effect of T94E). We also compared the effects of these mutants to wild type Tctex-1. We then performed co-IP experiments to detect the binding of KIM-1 to the different forms of Tctex-1 either before or after stimulation with apoptotic cells for 90 min. The phosphomimetic mutant of Tctex-1 (T94E) showed a significant decrease in the interaction with KIM-1 regardless of whether the cells were stimulated with apoptotic cells or not (Figures 8a and 8b). On the other hand, both wild type and unphosphorylated mimic mutant (T94A) forms of Tctex-1 bound to KIM-1 and showed no significant difference in their ability to interact with KIM-1. Next, we tested whether the phosphorylation status of Tctex-1 would have an effect on KIM-1-mediated efferocytosis. Following transfection of HEK-293 cells with KIM-1 and each individual Tctex-1 construct, cells were fed fluorescently-labelled apoptotic cells for 90 min and phagocytic ability was measured by flow cytometry (Figure 8c). Remarkably, no significant differences in phagocytic ability were seen between KIM-1-expressing HEK-293 cells that were transfected with either wild type, unphosphorylated mimic of Tctex-1 mutant (T94A), or the phosphomimetic mutant of Tctex-1 (T94E) (Figure 8d). In order to further confirm that there is no effect of phosphomimetic mutant of Tctex-1 on KIM-1-dependent phagocytosis, we performed an experiment where we rescued Tctex-1 expression in 769-P stably expressing shTctex-1 with

a different Tctex-1 construct (WT, T94A, T94E) for 48 hr and measured their protein expression using Western blotting (Figure 9a). As expected, the transfection rescued expression of Tctex-1 in these cells and did not affect KIM-1-expression. Next, we stimulated these cells with fluorescently-labelled apoptotic cells for 90 min and found that there was a significant decrease in KIM-1-medicated efferocytosis when compared to cells stably transfected with control shRNA (Figures 9b and 9c). However, all the different Tctex-1 constructs (WT, T94A, T94E) transfected into shTctex-1 cells were unable to rescue the phagocytic phenotype in shTctex-1 cells. In order to visualize whether these different DYNTL1 construct are active in the cells, we immunostained shTctex-1 cells transfected with different Tctex-1 construct (WT, T94A, T94E) with Alexa488-conjugated anti-flag antibody (staining for transfected Tctex-1) and Cy3-conjugated beta-tubulin stain (Figure 9d). As expected, Tctex-1 T94E construct showed a staining pattern that is independent of tubulin structure, as it is phosphomimic and does not bind to dynein. On the other hand, both Tctex-1 T94A and Tctex-1 WT colocalized with tubulin structures, as both forms of Tctex-1 retain their ability to bind to dynein which is part of microtubule structure. To rule out any toxic effects from our experimental strategy, we tested the viability of shTctex-1 cells transfected with these different constructs using Annexin V and PI staining (Supplementary Figure S3). There was no significant difference in cell death between cells with control shRNA, Tctex-1 shRNA, and Tctex-1 shRNA transfected with different Tctex-1 constructs. Altogether, these results argued that the phosphorylation of Tctex-1 at Threonine-94 affected the interaction between KIM-1 and Tctex-1, but did not impact KIM-1-mediated phagocytosis.

Tctex-1 regulates KIM-1-mediated phagocytosis through a Rho GTPase-independent pathway

The above experiments, suggested that Tctex-1 expression was crucial for KIM-1-dependent apoptotic cell-uptake. Tctex-1 has been shown previously to modulate the actin cytoskeleton through activation of Rac1 (Albert, Kim, & Birge, 2000; Campbell et al., 1998; Chuang et al., 2005) and RhoA (Conde et al., 2010; McIntire et al., 2001; Meiri et al., 2009). With regard to phagocytosis, it is well established that these Rho GTPases play important roles in actin cytoskeleton organization (Ridley, 2001; Ridley & Hall., 1992). Specifically, RhoA and Rac1 have been proposed to have opposing effects on the actin cytoskeleton and efferocytosis (Hall & Nobes, 2000; Meyer, Hunt, Schwesinger, & Denker, 2003; Mueller et al., 2002; Nakaya et al., 2006). We previously showed that inhibition of RhoA significantly increased KIM-1-dependent uptake of apoptotic cells via KIM-1 interaction with the heterotrimeric G-protein, Gα12 (Ismail et al., 2015, 2016). On the other hand, Rac1 was found to have a positive role in KIM-1-mediated phagocytosis as its inhibition lead to decrease in KIM-1-mediated phagocytosis. With this in mind, the level of Rac1 activity was measure following 769-P cell incubation with apoptotic cells over the course of phagocytosis (0–90 min). Surprisingly, Rac1 activity seemed to increase minimally during uptake of apoptotic cells (Figure 10a). To test whether Tctex-1 silencing modified the actin cytoskeleton via Rac1, we measured Rac1 activation of 769-P cells with Tctex-1 shRNA or control shRNA following stimulation with apoptotic cells. The level of Rac1 activation was not significantly altered following silencing of Tctex1-1 during the course of apoptotic cell-engulfment (Figure 10b). To test the role of RhoA, we first measured the level of active

RhoA during KIM-1-mediated phagocytosis. We found a steady increase in the level of active RhoA during the uptake process of apoptotic cells by 769-P cells with significant difference seen during the late stage of phagocytosis (90 min) (Figure 10c). This result was consistent with our previous data measuring the level of active RhoA during uptake of apoptotic cells in HEK-293 cells expressing human KIM-1 (Ismail et al., 2016). Moreover, upon silencing of Tctex-1 in 769-P cells (shTctex-1), we did not observe any change in level of active RhoA when compared to control shRNA cells, regardless whether cells were stimulated with apoptotic cells or not (Figure 10d). These data suggested that Tctex-1 does not regulate Rac1 or RhoA activation in cell culture model during KIM-1-dependent efferocytosis.

DISCUSSION

KIM-1 is a phosphatidylserine receptor that is specifically upregulated by tubular epithelial cells (TECs) during ischemic or toxic AKI and enables TECs to clear apoptotic and necrotic cell debris (Arai et al., 2016; Ichimura, Hung, Yang, Stevens, & Bonventre, 2004; Ichimura et al., 2008). In this paper, we explored the intracellular signaling pathways downstream of KIM-1. We identified a novel functional interaction between Tctex-1 (Chuang et al., 2005; Meiri et al., 2012) and KIM-1. We have shown that the interaction between KIM-1 and Tctex-1 is a dynamic process and dissipates during the later stages of apoptotic cell engulfment. Inhibition of actin and microtubule polymerization also restored KIM-1 binding to Tctex-1 during the later stages of phagocytosis suggesting that the cytoskeleton plays a role in this process. We also report a previously unknown and positive role of Tctex-1 in KIM-1-mediated efferocytosis, as knocking down Tctex-1 inhibited phagocytosis similar to effects seen by knocking-down KIM-1. Interestingly, our immunostaining experiments suggest that cellular Tctex-1 which associates with microtubules in the absence of KIM-1, dissociates from the microtubules as a result of KIM-1 expression. This phenomenon may be driven by KIM-1-dependent inhibition of Threonine 94 phosphorylation of Tctex-1 following efferocytosis. Indeed, we found (using the Thr-94 phosphomimetic mutant of Tctex-1) that phosphorylation of Tctex-1 at Threonine-94 diminishes interaction between KIM-1 and Tctex-1 regardless of whether apoptotic cells were added or not. Data presented in Figure 10 suggests that Tctex-1 likely mediates KIM-1 phagocytic function through a non-canonical pathway independent of RhoA and Rac1 GTPases.

The loss of interaction between KIM-1 and Tctex-1 during the later stages of phagocytosis suggests that Tctex-1 has a dynamic role in corpse engulfment. Recently, it was reported that TIM-1 (another name for KIM-1) undergoes dynamic cycling through clathrin-dependent vesicles to mediate the lysosomal degradation of NUR77 (Balasubramanian et al., 2012), a nuclear receptor implicated in apoptosis and cell survival (Machacek et al., 2009). Throughout our experiments, we did not find any evidence of Tctex-1 degradation during the entire period of phagocytosis (90 min) as determined by Western blot. Moreover, knocking down Tctex-1 in KIM-1-expressing cells did not affect apoptosis or necrosis. Given what is known about Tctex-1 in the trafficking of various cell-surface receptors (Machado et al., 2003; Mueller et al., 2002; Tai et al., 1998), it was surprising that Tctex-1 did not regulate KIM-1 trafficking to the cell-surface. This was evident from our examination of cell-surface expression of KIM-1 in Tctex-1 silenced cells.

The phosphorylation of Tctex-1 at Threonine-94 has been shown to promote Tctex-1 dissociation from the dynein light chain complex which is required to promote dynein-independent functions (Chuang et al., 2005; Li et al., 2011). For example, phosphorylation of Tctex-1 has been linked to enhanced neurite outgrowth activity (Chuang et al., 2005), such as ciliary disassembly, leading to cell cycle progression and S-phase entry for neural progenitor cells (Li et al., 2011). The change in Tctex-1 staining pattern when KIM-1 was silenced suggested that KIM-1 expression strongly influences the localization of Tctex-1. This change in localization from more cytosolic to tubulin-associated staining could be due to Thr-94 phosphorylation of Tctex-1 as seen in immunoprecipitation study following apoptotic cell-stimulation and silencing of KIM-1. The perplexing data with regards to the lack of an effect of the T94E Tctex-1 mutant on phagocytosis and the inability of wild type and T94A Tctex-1 mutant to rescue phagocytosis in Tctex-1 silenced cells is likely reflective of unimportance of Tctex-1 phosphorylation level in KIM-1-mediated phagocytosis. Alternatively, this could be explained by the presence of adequate endogenous Tctex-1 to overcome the effects of the mutants.

Cytoplasmic Tctex-1 has been shown to regulate microtubules and the actin cytoskeleton through activation of Rac1 and RhoA, respectively (Chuang et al., 2005; Meiri et al., 2012, 2014). Recently, it was shown that Tctex-1 sequesters a key Rho guanine exchange factor, GEF-H1 and tethers it to microtubules allowing Rac1 to execute its function unopposed by RhoA (McIntire et al., 2001; Meiri et al., 2012). Upon activation, Tctex-1 was shown to release GEF-H1 tethered to microtubules, allowing it to then activate RhoA by promoting GDP exchange for GTP. Because we previously demonstrated that Rac1 is required for KIM-1-dependent phagocytosis, we tested whether Tctex-1 relays its signaling through Rac1 in KIM-1-expressing cells. However, we failed to see any difference in the level of Rac1 activation upon silencing of Tctex-1. Thus, we propose that Tctex-1 may mediate efferocytosis independent of Rac1. Furthermore, we determined that RhoA is also not involved in mediating Tctex-1 phagocytic signaling during KIM-1-mediated efferocytosis. Moreover, we propose that other GTPases (e.g., cdc42) or non-GTPase pathways might affect Tctex-1-mediated phagocytic signaling (Conde et al., 2010). Interestingly, Tctex-1 has been shown to bind equally to small GTPase Rab3D for translocation to microtubules (Pavlos et al., 2011) and small GTPase RagA(Ras superfamily of small G proteins) for linking Tctex-1 to dynein motor complex (Merino-Gracia et al., 2015). We predict that maybe other small GTPases could interact with Tctex-1 following the apoptotic cells stimulation replacing KIM-1 and influencing Tctex-1 phosphorylation.

To our knowledge, this is the first study that has explored a physiological function for Tctex-1 in kidney cells, and moreover in efferocytosis. The logical next step would be to determine if Tctex-1 has any role in AKI or kidney repair. Given that Tctex-1 has been shown to be involved in regulating cilium resorption during neurogenesis (Li et al., 2011; Ridley & Hall, 1992), a potential mechanism for involvement in AKI might be through regulation of the cilium of renal TECs, which act as flow sensors (Kotsis et al., 2007). In fact, a number of human renal syndromes, including polycystic kidney disease, Bardet-Biedl syndrome and nephronophthisis (Balasubramanian et al., 2012), have been shown to involve dysfunctional cilia, a microtubule-based organelle. Our present work linking Tctex-1 to

KIM-1-mediated phagocytosis by TECs for the first time is likely to lead to new avenues of research into the role of Tctex-1 in AKI and other chronic kidney diseases.

Supplementary Material

Refer to Web version on PubMed Central for supplementary material.

ACKNOWLEDGMENTS

We would like to thank Dr. Ching-Hwa Sung (Weill Cornell Medical College, NY, USA) for kindly providing us with plasmids encoding wild type and mutant (T94E, T94A) Txtex-1 (pCS982, pCS1034, and pCS1035) and Dr. Robert Rottapel (University of Toronto, Toronto, Canada) for providing us with plasmids encoding shRNA against Tctex-1. This work was supported by operating grants from the Canadian Institutes of Health Research Grant (HDK 232429 and 244945) and Western University. O.I. was the recipient of a Lawson Research Institute IRF studentship. L.G. was supported by a KRESCENT New Investigator Award. J.V.B. was supported by grants from the National Institutes of Health (NIH R37DK039773 and R01DKD07238).

Funding information

Canadian Institutes of Health Research, Grant numbers: HDK232429, HDK244945

Abbreviation:

ACs	apoptotic cells
AKI	acute kidney injury
HEK-293	human embryonic kidney-293; human renal adenocarcinoma cell lines (769-P)
KIM-1	kidney injury molecule-1 (human)
Kim-1	kidney injury molecule-1 (mouse)
pHrodo	pH-sensitive dye pHrodo™ Red succinimidyl ester
Tctex-1	dynein light chain Tctex-type 1
Tctex-1	t-Complex testis-expressed-1
Tctex-1-WT	wild type flag-tagged Tctex-1
Tctex-1-T94A	non-phosphorylated mimic flag-tagged Tctex-1
Tctex-1-T94E	phosphorylated mimic flag-tagged Tctex-1
TECs	tubular epithelial cells

REFERENCES

Albert ML, Pearce SF, Francisco LM, Sauter B, Roy P, Silverstein RL, & Bhardwaj N (1998). Immature dendritic cells phagocytose apoptotic cells via alphavbeta5 and CD36, and cross-present antigens to cytotoxic T lymphocytes. The Journal of Experimental Medicine, 188(7), 1359–1368.9763615

Albert ML, Kim JI, & Birge RB (2000). alphavbeta5 integrin recruits the Crkll-Dock180-rac1 complex for phagocytosis of apoptotic cells. Nature Cell Biology, 2(12), 899–905.11146654

Ambivero CT, Cilenti L, Main S, & Zervos AS (2014). Mulan E3 ubiquitin ligase interacts with multiple E2 conjugating enzymes and participates in mitophagy by recruiting GABARAP. Cell Signal, 26(12), 2921–2929.25224329

Arai S, Kitada K, Yamazaki T, Takai R, Zhang X, Tsugawa Y, … Miyazaki T (2016). Apoptosis inhibitor of macrophage protein enhances intraluminal debris clearance and ameliorates acute kidney injury in mice. Nature Medicine, 22(2), 183–193.

Bailly V, Zhang Z, Meier W, Cate R, Sanicola M, & Bonventre JV (2002). Shedding of kidney injury molecule-1, a putative adhesion protein involved in renal regeneration. The Journal of Biological Chemistry, 277(12138159), 39739–39748.12138159

Balasubramanian S, Kota SK, Kuchroo VK, Humphreys BD, & Strom TB (2012). TIM family proteins promote the lysosomal degradation of the nuclear receptor NUR77. Science Signaling, 5(254), ra90.23233528

Barton NR, & Goldstein LS (1996). Going mobile: Microtubule motors and chromosome segregation. Proceedings of the National Academy of Sciences of the United States of America, 93(5), 1735–1742.8700828

Binne LL, Scott ML, & Rennert PD (2007). Human TIM-1 associates with the TCR complex and up-regulates T cell activation signals. The Journal of Immunology, 178(7), 4342–4350.17371991

Campbell KS, Cooper S, Dessing M, Yates S, & Buder A (1998). Interaction of p59fyn kinase with the dynein light chain, Tctex-1, and colocalization during cytokinesis. The Journal of Immunology, 161-(9712037), 1728–1737.9712037

Chimini G, & Chavrier P (2000). Function of Rho family proteins in actin dynamics during phagocytosis and engulfment. Nature Cell Biology, 2(10), E191–E196.11025683

Chuang JZ, Yeh TY, Bollati F, Conde C, Canavosio F, Caceres A, & Sung CH (2005). The dynein light chain Tctex-1 has a dynein-independent role in actin remodeling during neurite outgrowth. Developmental Cell, 9(1), 75–86.15992542

Conde C, Arias C, Robin M, Li A, Saito M, Chuang JZ, … Caceres A (2010). Evidence for the involvement of Lfc and Tctex-1 in axon formation. Journal of Neuroscience, 30(19), 6793–6800.20463241

Curtiss ML, Hostager BS, Stepniak E, Singh M, Manhica N, Knisz J, … Rothman PB (2011). Fyn binds to and phosphorylates T cell immunoglobulin and mucin domain-1 (Tim-1). Molecular Immunology, 48(12–13), 1424–1431.21513984

Duvall E, Wyllie AH, & Morris RG (1985). Macrophage recognition of cells undergoing programmed cell death (apoptosis). Immunology, 56(2), 351–358.3876985

Elliott MR, Zheng S, Park D, Woodson RI, Reardon MA, Juncadella IJ, … Ravichandran KS (2010). Unexpected requirement for ELMO1 in clearance of apoptotic germ cells in vivo. Nature, 467(7313), 333–337.20844538

Finnemann SC, Bonilha VL, Marmorstein AD, & Rodriguez-Boulan E (1997). Phagocytosis of rod outer segments by retinal pigment epithelial cells requires alpha(v)beta5 integrin for binding but not for internalizetion. Proceedings of the National Academy of Sciences of the United States of America, 94(24), 12932–12937.9371778

Freeman SA, & Grinstein S (2014). Phagocytosis: receptors, signal integration, and the cytoskeleton. Immunological Reviews, 262(1), 193–215.25319336

Gauthier-Fisher A, Lin DC, Greeve M, Kaplan DR, Rottapel R, & Miller FD (2009). Lfc and Tctex-1 regulate the genesis of neurons from cortical precursor cells. Nature Neuroscience, 12(6), 735–744.19448628

Hall A, & Nobes CD (2000). Rho GTPases: molecular switches that control the organization and dynamics of the actin cytoskeleton. Philosophical Transactions of the Royal Society of London B Biological Sciences, 355(1399), 965–970.11128990

Hartwig JH, Davies WA, & Stossel TP (1977). Evidence for contractile protein translocation in macrophage spreading, phagocytosis, and phagolysosome formation. The Journal of Cell Biology, 75(3), 956–967.925089

Harrison RE, & Grinstein S (2002). Phagocytosis and the microtubule cytoskeleton. Biochemistry and Cell Biology, 80(5), 509–515.12440692

Hirokawa N (1998). Kinesin and dynein superfamily proteins and the mechanism of organelle transport. Science, 279(5350), 519–526.9438838

Hirokawa N, Noda Y, & Okada Y (1998). Kinesin and dynein superfamily proteins in organelle transport and cell division. Current Opinion in Cell Biology, 10(9484596), 60–73.9484596

Ichimura T, Asseldonk EJ, Humphreys BD, Gunaratnam L, Duffield JS, & Bonventre JV (2008). Kidney injury molecule-1 is a phosphatidylserine receptor that confers a phagocytic phenotype on epithelial cells. Journal of Clinical Investigation, 118(5), 1657–1668.18414680

Ichimura T, Bonventre JV, Bailly V, Wei H, Hession CA, Cate RL, & Sanicola M (1998). Kidney injury molecule-1 (KIM-1), a putative epithelial cell adhesion molecule containing a novel immunoglobulin domain, is up-regulated in renal cells after injury. The Journal of Biological Chemistry, 273(7), 4135–4142.9461608

Ichimura T, Hung CC, Yang SA, Stevens JL, & Bonventre JV (2004). Kidney injury molecule-1: A tissue and urinary biomarker for nephrotoxicant-induced renal injury. American Journal of Physiology-Renal Physiology, 286(3), F552–F563.14600030

Ismail OZ, Zhang X, Wei J, Haig A, Denker BM, Suri RS, … Gunaratnam L (2015). Kidney injury molecule-1 protects against Galpha12 activation and tissue damage in renal ischemia-reperfusion injury. The American Journal of Pathology, 185(5), 1207–1215.25759266

Ismail OZ, Zhang X, Bonventre JV, & Gunaratnam L (2016). G protein alpha12 (Galpha12) is a negative regulator of kidney injury molecule-1-mediated efferocytosis. American Journal of Physiology Renal Physiology, 310(7), F607–F620.26697979

Juncadella IJ, Kadi A, Sharma AK, Shim YM, Hochreiter-Hufford A, Borish L, & Ravichandran KS (2013). Apoptotic cell clearance by bronchial epithelial cells critically influences airway inflammation. Nature, 493(7433), 547–551.23235830

Kerr JF (2002). History of the events leading to the formulation of the apoptosis concept. Toxicology, 181–182, 471–474.

Kerr JF, Wyllie AH, & Currie AR (1972). Apoptosis: A basic biological phenomenon with wide-ranging implications in tissue kinetics. British Journal of Cancer, 26(4), 239–257.4561027

King SM, Dillman JF, Benashski SE, Lye RJ, Patel-King RS, & Pfister KK (1996). The mouse t-complex-encoded protein Tctex-1 is a light chain of brain cytoplasmic dynein. The Journal of Biological Chemistry, 271(50), 32281–32287.8943288

Kobayashi N, Karisola P, Pena-Cruz V, Dorfman DM, Jinushi M, Umetsu SE, … Freeman GJ (2007). TIM-1 and TIM-4 glycoproteins bind phosphatidylserine and mediate uptake of apoptotic cells. Immunity, 27(6), 927–940.18082433

Kotsis F, Nitschke R, Boehlke C, Bashkurov M, Walz G, & Kuehn EW (2007). Ciliary calcium signaling is modulated by kidney injury molecule-1 (Kim1). Pflügers Archiv, 453(6), 819–829.17205356

Lader E, Ha HS, O'Neill M, Artzt K, & Bennett D (1989). Tctex-1: A candidate gene family for a mouse t complex sterility locus. Cell, 58(5), 969–979.2570638

Li A, Saito M, Chuang JZ, Tseng YY, Dedesma C, Tomizawa K, … Sung CH (2011). Ciliary transition zone activation of phosphorylated Tctex-1 controls ciliary resorption, S-phase entry and fate of neural progenitors. Nature Cell Biology, 13(4), 402–411.21394082

Machacek M, Hodgson L, Welch C, Elliott H, Pertz O, Nalbant P, … Danuser G (2009). Coordination of Rho GTPase activities during cell protrusion. Nature, 461(7260), 99–103.19693013

Machado RD, Rudarakanchana N, Atkinson C, Flanagan JA, Harrison R, Morrell NW, & Trembath RC (2003). Functional interaction between BMPR-II and Tctex-1, a light chain of Dynein, is isoform-specific and disrupted by mutations underlying primary pulmonary hypertension. Human Molecular Genetics, 12(24), 3277–3286.14583445

Martin CB, Mahon GM, Klinger MB, Kay RJ, Symons M, Der CJ, & Whitehead IP (2001). The thrombin receptor, PAR-1, causes transformation by activation of Rho-mediated signaling pathways. Oncogene, 20(16), 1953–1963.11360179

McIntire JJ, Umetsu SE, Akbari O, Potter M, Kuchroo VK, Barsh GS, … DeKruyff RH (2001). Identification of Tapr (an airway hyperreactivity regulatory locus) and the linked Tim gene family. Nature Immunology, 2(12), 1109–1116.11725301

Meiri D, Greeve MA, Brunet A, Finan D, Wells CD, LaRose J, & Rottapel R (2009). Modulation of Rho guanine exchange factor Lfc activity by protein kinase A-mediated phosphorylation. Molecular and Cellular Biology, 29(21), 5963–5973.19667072

Meiri D, Marshall CB, Greeve MA, Kim B, Balan M, Suarez F, … Rottapel R (2012). Mechanistic insight into the microtubule and actin cytoskeleton coupling through dynein-dependent RhoGEF inhibition. Molecular Cell, 45(5), 642–655.22405273

Meiri D, Marshall CB, Mokady D, LaRose J, Mullin M, Gingras AC, … Rottapel R (2014). Mechanistic insight into GPCR-mediated activation of the microtubule-associated RhoA exchange factor GEF-Hl. Nature Communications, 5, 4857.

Merino-Gracia J, Garcia-Mayoral MF, Rapali P, Valero RA, Bruix M, & Rodriguez-Crespo I (2015). DYNLT (Tctex-1) forms a tripartite complex with dynein intermediate chain and RagA, hence linking this small GTPase to the dynein motor. The FEBS Journal, 282(20), 3945–3958.26227614

Meyer TN, Hunt J, Schwesinger C, & Denker BM (2003). Galpha12 regulates epithelial cell junctions through Src tyrosine kinases. American Journal of Physiology, 285(5), C1281–C1293.12890651

Miyanishi M, Tada K, Koike M, Uchiyama Y, Kitamura T, & Nagata S (2007). Identification of Tim4 as a phosphatidylserine receptor. Nature, 450(7168), 435–439.17960135

Monks J, Geske FJ, Lehman L, & Fadok VA (2002). Do inflammatory cells participate in mammary gland involution?. Journal of Mammary Gland Biology and Neoplasia, 7(2), 163–176.12463737

Mueller S, Cao X, Welker R, & Wimmer E (2002). Interaction of the poliovirus receptor CD155 with the dynein light chain Tctex-1 and its implication for poliovirus pathogenesis. The Journal of Biological Chemistry, 277(10), 7897–7904.11751937

Nakaya M, Tanaka M, Okabe Y, Hanayama R, & Nagata S (2006). Opposite effects of rho family GTPases on engulfment of apoptotic cells by macrophages. The Journal of Biological Chemistry, 281(13), 8836–8842.16439364

Palmer KJ, MacCarthy-Morrogh L, Smyllie N, & Stephens DJ (2011). A role for Tctex-1 (DYNLT1) in controlling primary cilium length. European journal of cell biology, 90(10), 865–871.21700358

Park D, Tosello-Trampont AC, Elliott MR, Lu M, Haney LB, Ma Z, … Ravichandran KS (2007). BAI1 is an engulfment receptor for apoptotic cells upstream of the ELMO/Dockl80/Rac module. Nature, 450(7168), 430–434.17960134

Patel VA, Lee DJ, Feng L, Antoni A, Lieberthal W, Schwartz JH, … Levine JS (2010). Recognition of apoptotic cells by epithelial cells: Conserved versus tissue-specific signaling responses. The Journal of Biological Chemistry, 285(3), 1829–1840.19910463

Pavlos NJ, Cheng TS, Qin A, Ng PY, Feng HT, Ang ES, … Xu J (2011). Tctex-1, a novel interaction partner of Rab3D, is required for osteoclastic bone resorption. Molecular and Cellular Biology, 31(7), 1551–1564.21262767

Ravichandran KS, & Lorenz U (2007). Engulfment of apoptotic cells: Signals for a good meal. Nature Reviews Immunology, 7(12), 964–974.

Ren Y, & Savill J (1998). Apoptosis: The importance of being eaten. Cell Death & Differentiation, 5(7), 563–568.10200510

Ridley AJ, & Hall A (1992). Distinct patterns of actin organization regulated by the small GTP-binding proteins Rac and Rho. Cold Spring Harbor Symposia on Quantitative Biology, 57, 661–671.1339704

Ridley AJ (2001). Rho family proteins: coordinating cell responses. Trends in Cell Biology, 11(12), 471–477.11719051

Sachdev P, Menon S, Kastner DB, Chuang JZ, Yeh TY, Conde C, … Sakmar TP (2007). G protein beta gamma subunit interaction with the dynein light-chain componentTctex-1 regulates neurite outgrowth. The EMBO Journal, 26(11), 2621–2632.17491591

Santiago C, Ballesteros A, Tami C, Martinez-Munoz L, Kaplan GG, & Casasnovas JM (2007). Structures of T Cell immunoglobulin mucin receptors 1 and 2 reveal mechanisms for regulation of immune responses by the TIM receptor family. Immunity, 26(3), 299–310.17363299

Schroer TA (1994). Structure, function and regulation of cytoplasmic dynein. Current Opinion in Cell Biology, 6(1), 69–73.8167028

Shiratsuchi A, Umeda M, Ohba Y, & Nakanishi Y (1997). Recognition of phosphatidylserine on the surface of apoptotic spermatogenic cells and subsequent phagocytosis by Sertoli cells of the rat. The Journal of Biological Chemistry, 272(4), 2354–2358.8999945

Song Y, Benison G, Nyarko A, Hays TS, & Barbar E (2007). Potential role for phosphorylation in differential regulation of the assembly of dynein light chains. The Journal of Biological Chemistry, 282(23), 17272–17279.17428790

Steuer ER, Wordeman L, Schroer TA, & Sheetz MP (1990). Localization of cytoplasmic dynein to mitotic spindles and kinetochores. Nature, 345(6272), 266–268.2139718

Tai AW, Chuang JZ, Bode C, Wolfrum U, & Sung CH (1999). Rhodopsin's carboxy-terminal cytoplasmic tail acts as a membrane receptor for cytoplasmic dynein by binding to the dynein light chain Tctex-1. Cell, 97(7), 877–887.10399916

Tai AW, Chuang JZ, & Sung CH (1998). Localization of Tctex-1, a cytoplasmic dynein light chain, to the Golgi apparatus and evidence for dynein complex heterogeneity. The Journal of Biological Chemistry, 273(9677391), 19639–19649.9677391

Tai AW, Chuang JZ, & Sung CH (2001). Cytoplasmic dynein regulation by subunit heterogeneity and its role in apical transport. The Journal of Cell Biology, 153(7), 1499–1509.11425878

Toda S, Hanayama R, & Nagata S (2012). Two-step engulfment of apoptotic cells. Molecular and Cellular Biology, 32(1), 118–125.22037761

Vandivier RW, Henson PM, & Douglas IS (2006). Burying the dead: The impact of failed apoptotic cell removal (efferocytosis) on chronic inflammatory lung disease. Chest, 129(6), 1673–1682.16778289

Wang H, Bedford FK, Brandon NJ, Moss SJ, & Olsen RW (1999). GABA(A)-receptor-associated protein links GABA(A) receptors and the cytoskeleton. Nature, 397(6714), 69–72.9892355

Wong K, Pertz O, Hahn K, & Bourne H (2006). Neutrophil polarization: spatiotemporal dynamics of RhoA activity support a self-organizing mechanism. Proceedings of the National Academy of Sciences of the United States of America, 103(10), 3639–3644.16537448

Wyllie AH, Kerr JF, & Currie AR (1980). Cell death: The significance of apoptosis. International Review of Cytology, 68, 251–306.7014501

Yang L, Brooks CR, Xiao S, Sabbisetti V, Yeung MY, Hsiao LL, … Bonventre JV (2015). KIM-1-mediated phagocytosis reduces acute injury to the kidney. Journal of Clinical Investigation, 125(4), 1620–1636.25751064

Yano H, Cong F, Birge RB, Goff SP, & Chao MV (2000). Association of the Abl tyrosine kinase with the Trk nerve growth factor receptor. Journal of Neuroscience Research, 59(3), 356–364.10679771

Yeh TY, Peretti D, Chuang JZ, Rodriguez-Boulan E, & Sung CH (2006). Regulatory dissociation of Tctex-1 light chain from dynein complex is essential for the apical delivery of rhodopsin. Traffic, 7(11), 1495–1502.16956385

Zervos AS, Gyuris J, & Brent R (1993). Mxil, a protein that specifically interacts with Max to bind Myc-Max recognition sites. Cell, 72(2), 223–232.8425219

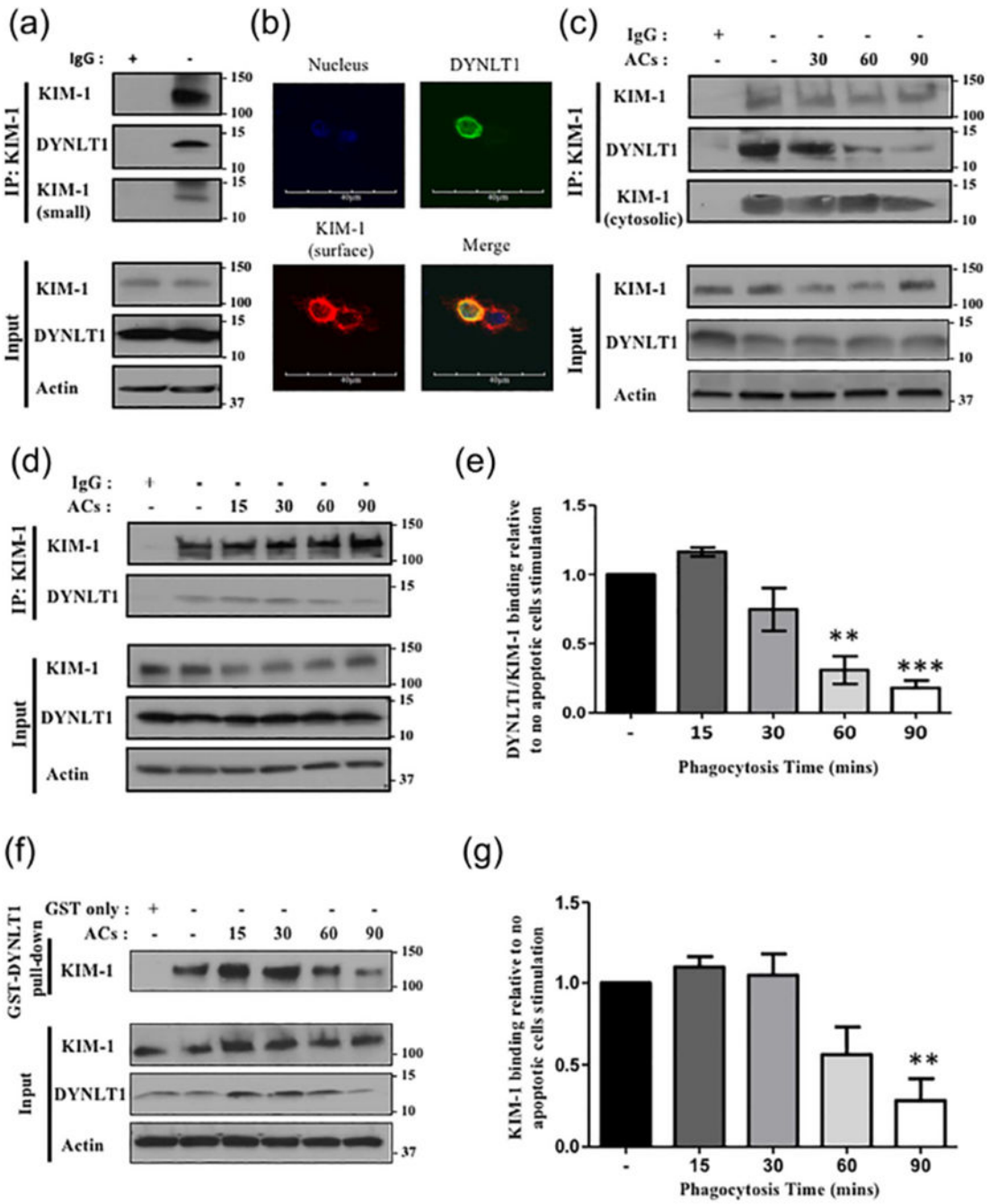

FIGURE 1.

KIM-1 interacts with Tctex-1 during the early stages of phagocytosis, (a) Human embryonic kidney-293 (HEK-293) cells transfected with human KIM-1-GFP and flag-tagged Tctex-1 were lysed for immunoprecipitation (IP) using antibody against the cytosolic domain of KIM-1 or control non-specific mouse immunoglobulin antibody (IgG). (b) Cells in A were visualized for interaction using immunostaining for KIM-1 (red) and Tctex-1(green) as indicated in the experimental procedures section. Nuclei was stained with DAPI (blue) (600×, bar represents 40 μm). (c) Cells in A were stimulated with apoptotic cells (ACs) for

various time points (minutes) and IP was performed using KIM-1 antibody or control mouse IgG. (d) 769-P cells were stimulated with apoptotic cells and IP was performed similarly to C. (e) The level of bound Tctex-1 to KIM-1 was determined based on densitometry values obtained by Western blotting ($n = 3$, $^{**}p < 0.01$, $^{***}p < 0.001$, one-way ANOVA). (f) GST and GST- Tctex-1 pull-down was performed on 769-P cells that were left unstimulated or stimulated with apoptotic cells for indicated time (in minutes), (g) The level of KIM-1 bound to GST- Tctex-1 was determined based on densitometric values obtained from Western blotting ($n = 3$, $^{**}p < 0.01$, one-way ANOVA). All samples in (a), (c), (d), and (f) were analyzed by SDS-PAGE followed by immunoblotting with antibodies against KIM-1, Tctex-1, and actin. The input lane represents 5% of the lysate. The data represents three independent experiments

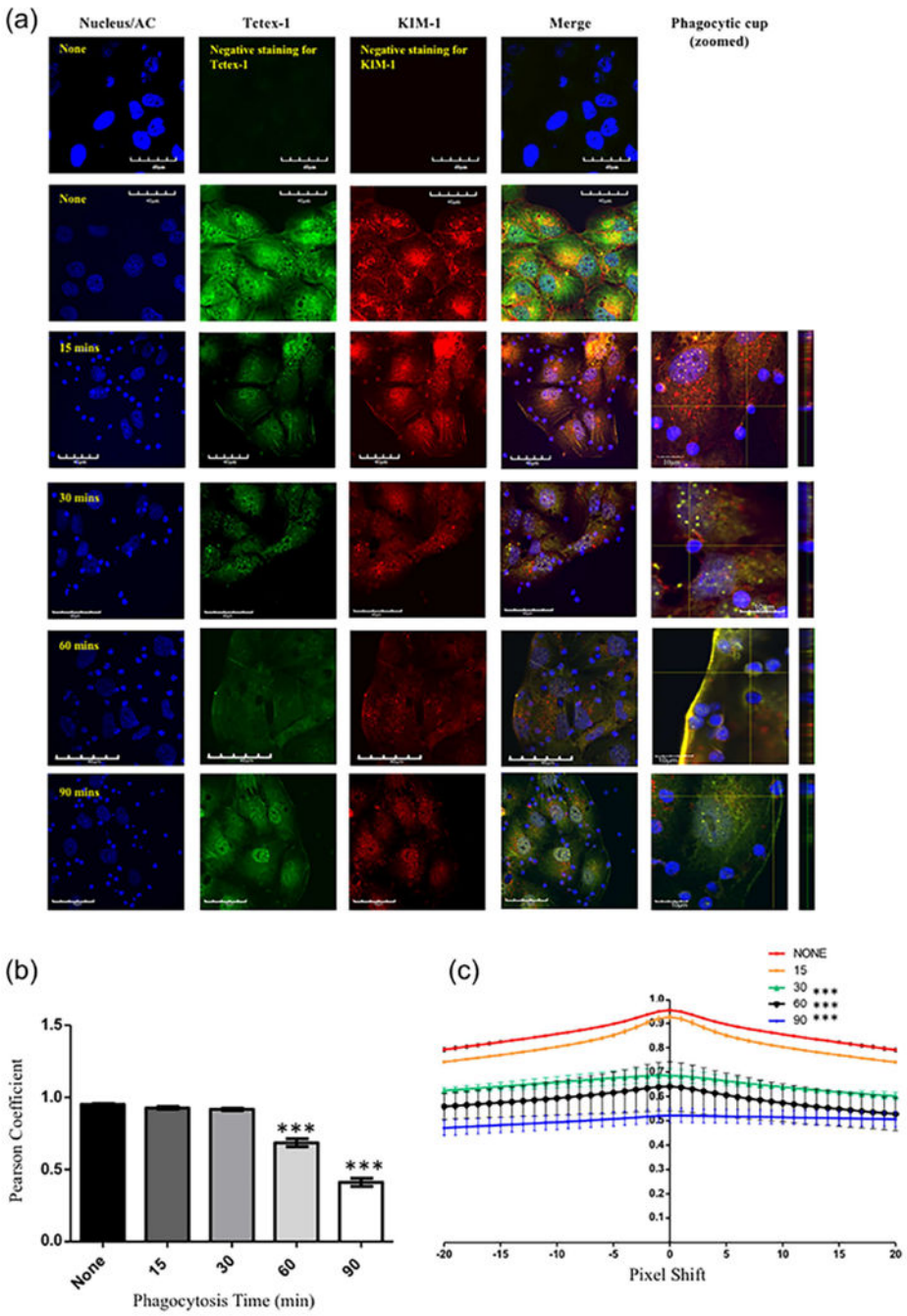

FIGURE 2.

KIM-1 co-localizes with Tctex-1/DYNLT-1 during the early stages of phagocytosis. (a) 769-P cells were stimulated with apoptotic cells (blue) for various time points. Both KIM-1 and Tctex-1 were visualized using immunostaining for Tctex-1 (green) and KIM-1 (red) using Alexa-488 and Alex-555 labeled secondary antibodies as indicated in the experimental procedures section. Nuclei was counter-stained with DAPI (blue) (600×, bar represents 40 μm). Further magnification is shown for the phagocytic cup formed by KIM-1 and apoptotic cells (bar represents 10 μm). Vertical lines appearing at 90 min of apoptotic cells-stimulation

are suggestive of Tctex-1 trafficking along microtubules as indicated previously (47). (b) Images of colocalization of both KIM-1 and Tctex-1 over the time course of phagocytosis were analyzed using Pearson's coefficient ($n = 3$, ***$p < 0.001$, one-way ANOVA). (c) Colocalization of both KIM-1 and Tctex-1 during the course of uptake of apoptotic cells was analyzed using the Van Steensel's approach, where the cross correlation function (CCF) was calculated with a pixel shift of ±20 ($n = 3$, ***$p < 0.001$ compared to none stimulated cells, one-way ANOVA). Quantification of colocalization score was assessed based on three random fields per sample and was done in three independent experiments

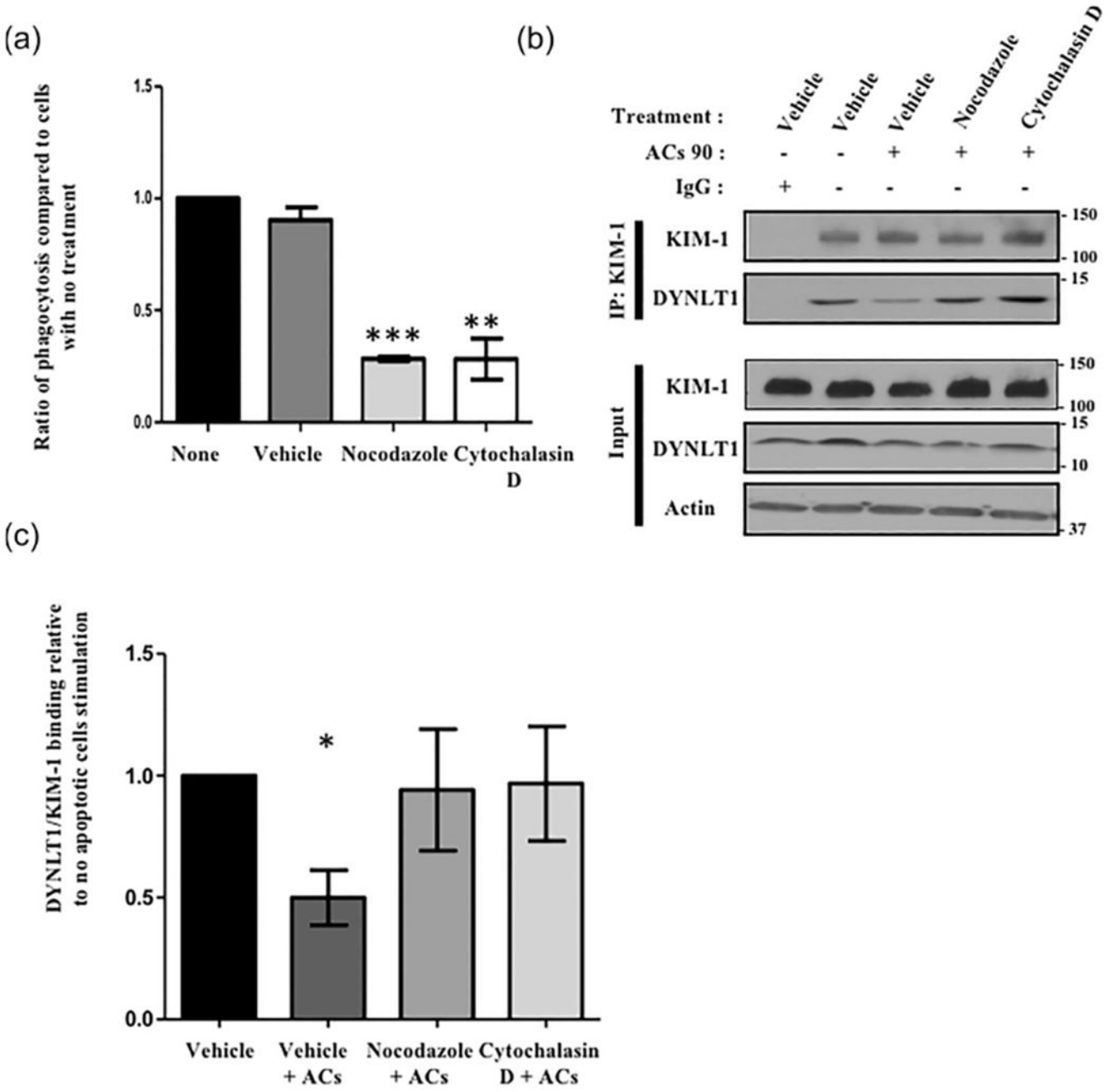

FIGURE 3.

Inhibition of KIM-1-mediated phagocytosis by inhibiting actin and microtubule dynamics restores the interaction between Tctex-1 and KIM-1 following apoptotic cell uptake. (a) 769-P cells were treated with vehicle (DMSO), nocodazole (10 μM) or cytochalasin D (1 μM) prior to adding fluorescently labeled apoptotic cells (pHrodo red) for 90 min (ACs 90). The percentage of uptake of the apoptotic cells as indicated by high pHrodo red fluorescence was measured by flow cytometry ($n = 3$, $^{***}p < 0.001$, unpaired t-test). (b) Cells in (a) were either unstimulated or stimulated with apoptotic cells for 90 min and used for immunoprecipitation (IP) using KIM-1 antibody as described in the experimental procedures

section. All samples were analyzed by SDS-PAGE followed by immunoblotting with antibodies against KIM-1, Tctex-1, and actin. The input lane represents 5% of the lysate. (c) Level of Tctex-1 bound to KIM-1 following different treatments was determined based on densitometric values obtained from three independent Western blotting experiments ($n = 3$, $^{*}p < 0.05$, unpaired t-test)

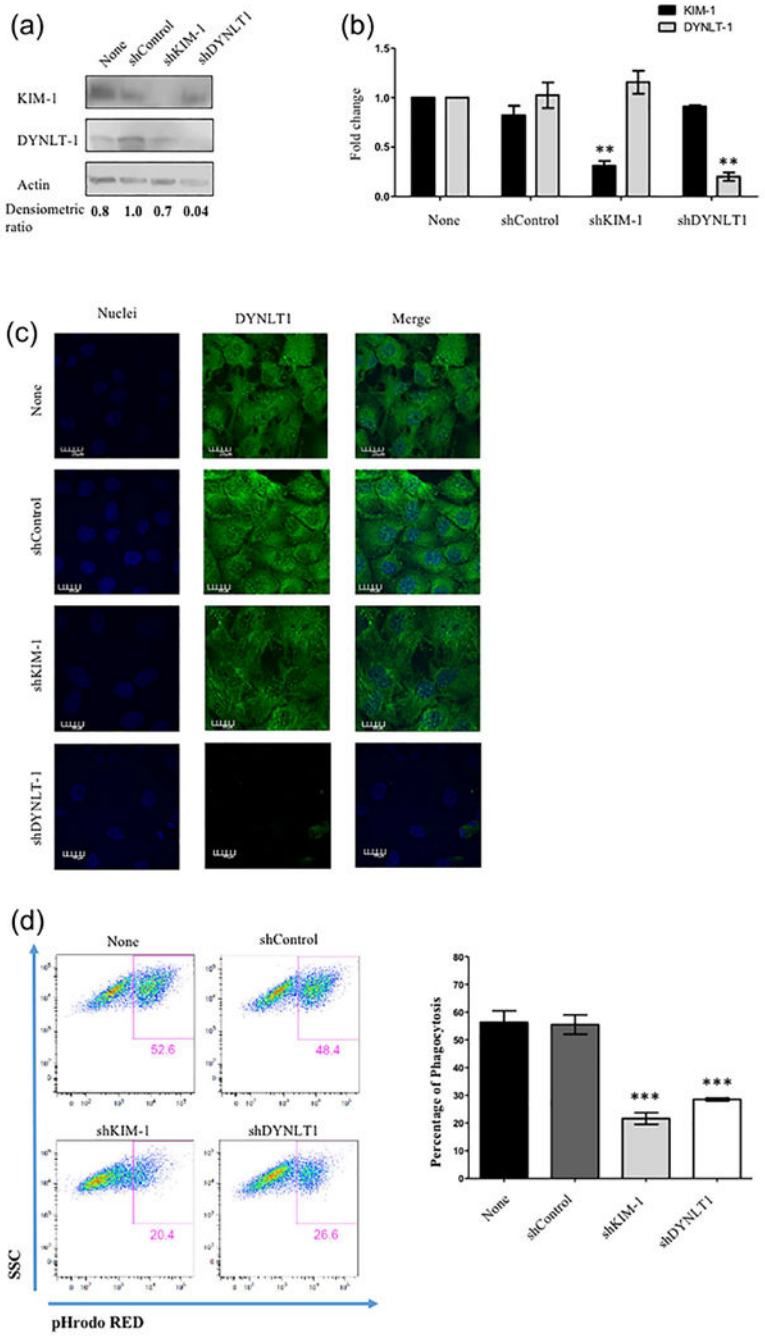

FIGURE 4.

TCTEX-1 expression is required for KIM-1-mediated efferocytosis. (a) 769-P cells were left untransfected or stably transfected with either control shRNA (shControl), KIM-1 shRNA (shKIM-1), or Tctex-1 shRNA (sh Tctex-1). Cells were lysed and protein levels of shTCTEX-1, KIM-1, and actin were determined by immunoblotting. (b) RT-qPCR analysis of the expression levels of KIM-1 and Tctex-1 in different cells presented in (a). The qPCR results were normalized to GAPDH and compared with the expression level in 769P untransfected (none) ($n = 3$, ** $p < 0.01$, unpaired t-test). (c) Cells in (a) were grown on

glass coverslips and stained for endogenous TCTEX-1 using immunostaining for Tctex-1 (green) via AlexaFluor-488 labeled secondary antibodies as indicated in the experimental procedures section (600×, bar represents 20 μm). (d) Cells were fed fluorescently labeled apoptotic cells (pHrodo red) for 90 min. The percentage of uptake of apoptotic cells was determined by flow cytometry as shown in the plots of side-scatter (SSC) versus pHrodo red (apoptotic cells). The percentage of phagocytosis was measured by flow cytometry and shown as representation of four independent experiments ($n = 4$, $^{***}p < 0.001$, unpaired *t*-test)

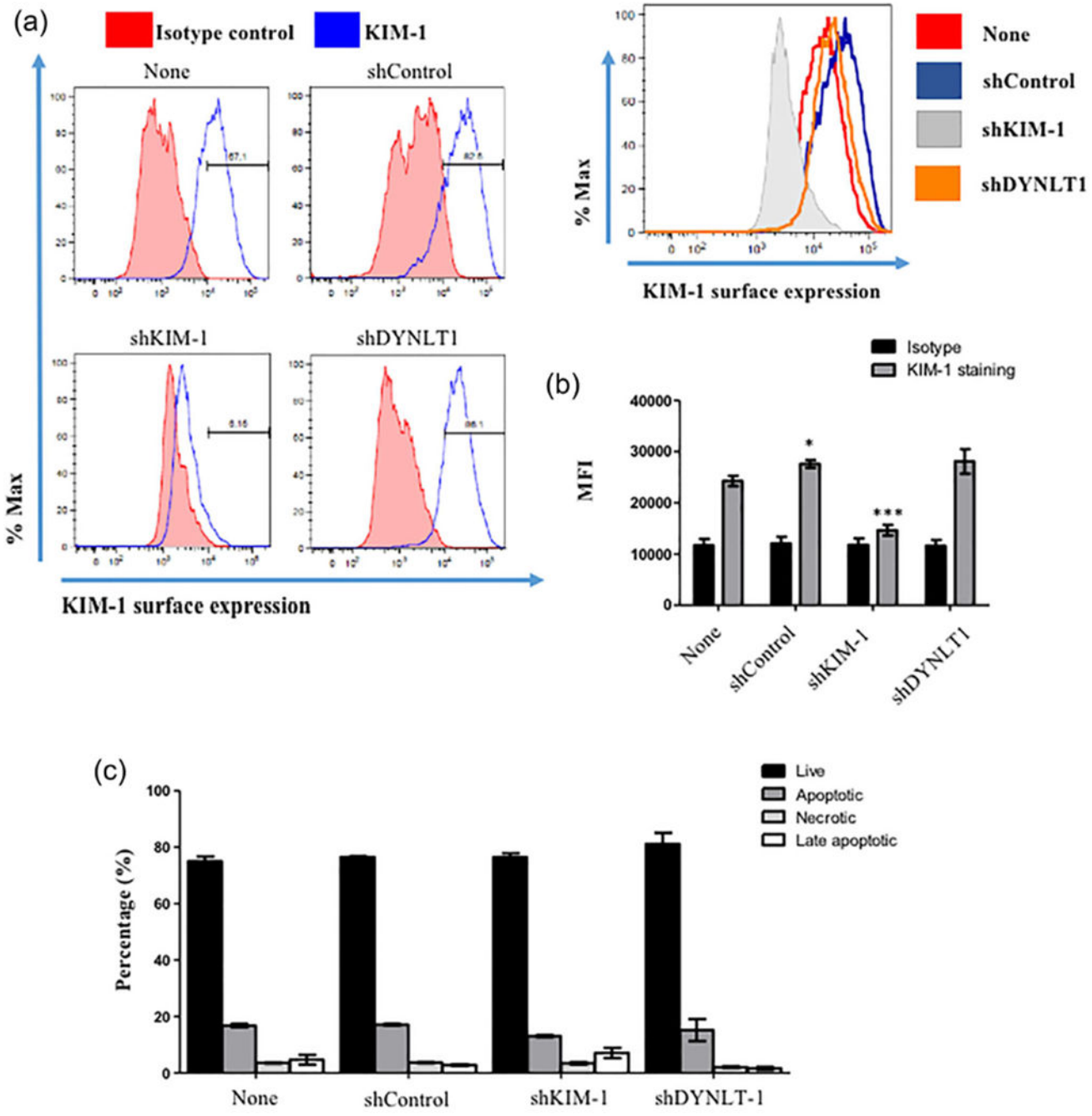

FIGURE 5.

Tctex-1 Knockdown does not affect KIM-1-surface expression or cell viability. (a) 769-P cells were left untransfected or stably transfected with either control shRNA, KIM-1 shRNA, or Tctex-1 shRNA. Cells were stained for surface KIM-1 using PE-conjugated anti-KIM 1 antibody and its isotype control, without permeabilization. The level of KIM-1-surface expression was determined by flow cytometry as shown by KIM-1-surface expression hectographs. (b) Representative graph of the mean fluorescence intensity (MFI) of the flow cytometry data from (a) was shown as representative of four independent experiments ($n = 4$,

*$p < 0.05$ compared to none, **$p < 0.001$ compared to none and shControl, unpaired t-test). (c) Cells in (a) were stained with PI and FITC-conjugated Annexin V to determine the percentage of live (negative Annexin V and PI), apoptotic (positive Annexin V only), necrotic (positive PI only), and late apoptotic (positive for Annexin V and PI) cells. The graph represents four independent experiments ($n = 4$, no significant difference observed between different types of cells for each type of cell death/viability)

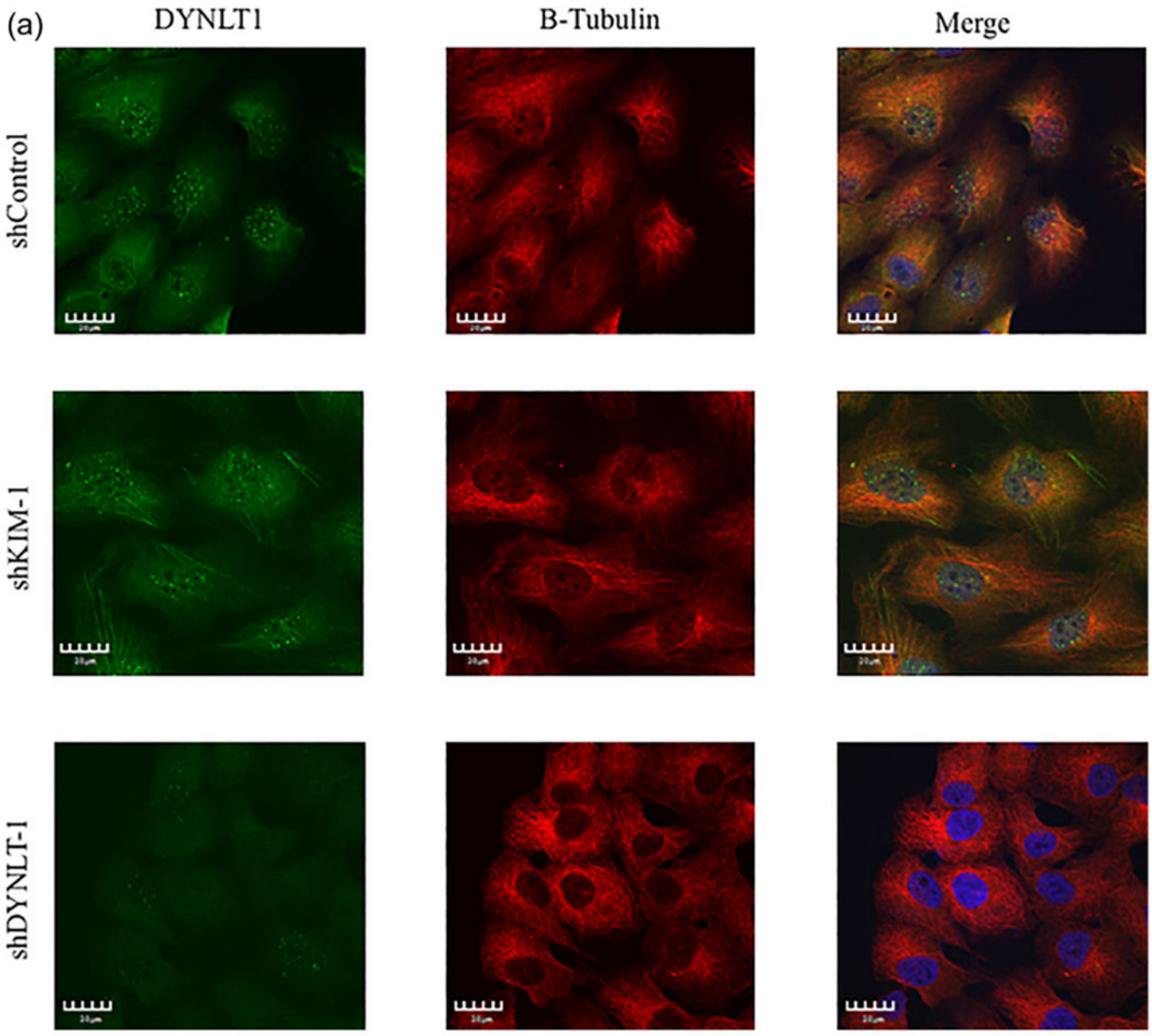

FIGURE 6.

Tctex-1 localization changes following KIM-1 knockdown. (a) 769-P cells were stably transfected with either control shRNA, KIM-1 shRNA, or Tctex-1 shRNA. Cells were fixed and permeabilized for immunostaining for Tctex-1 and Cy3-conjugated Beta-tubulin. Tctex-1 staining was visualized using AlexaFlour-488 secondary antibody as indicated in method section. Result represent three independent experiment (600×, bar represents 20 μm)

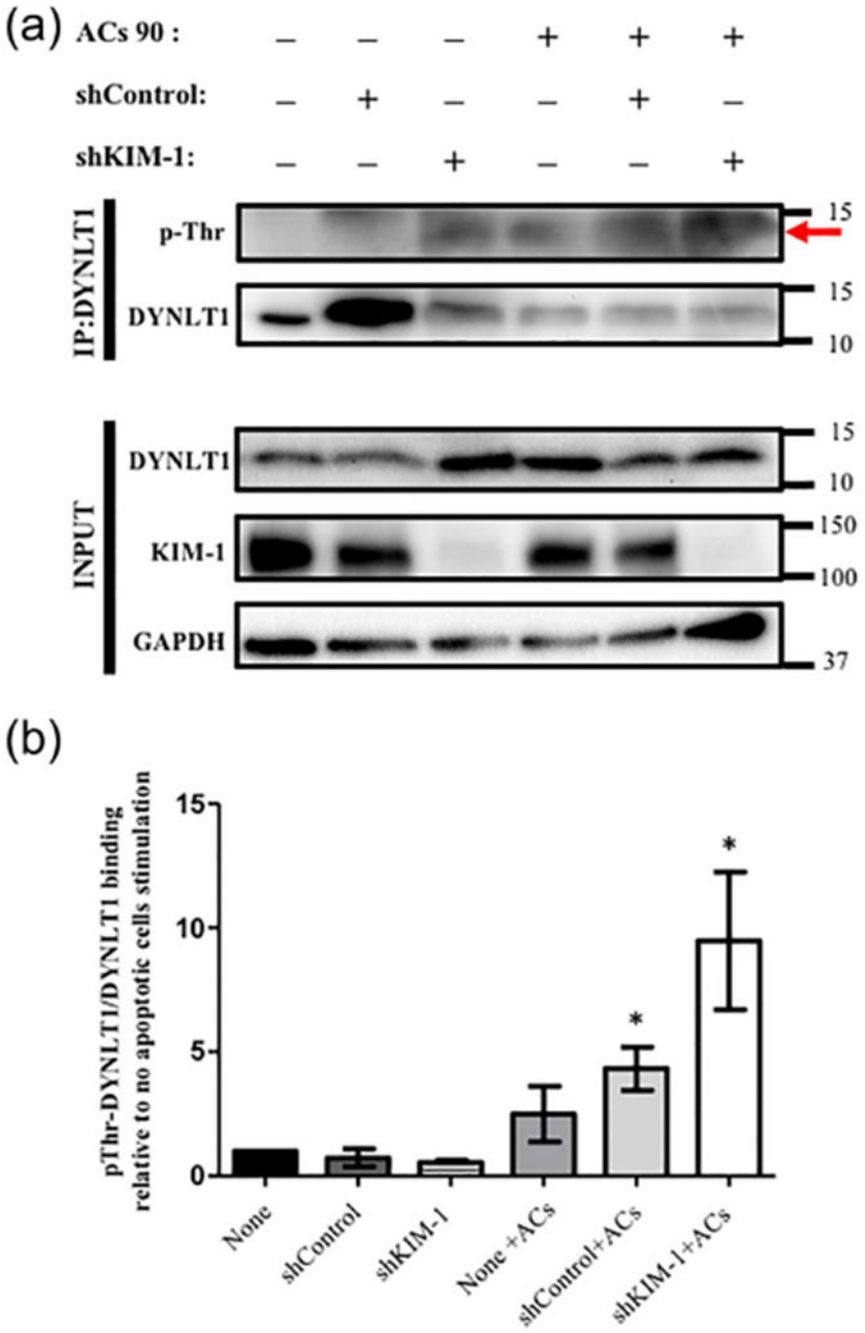

FIGURE 7.

Threonine phosphorylation of endogenous DYNLT1 appears to be stimulated by KIM-1-mediated uptake of apoptotic cells and enhanced in KIM-1-silencing. (a) 769-P cells were left untransfected or stably transfected with either control shRNA or KIM-1 shRNA. Cells were lysed for immunoprecipitation (IP) using antibody against DYNLT1. The samples analyzed by SDS-PAGE followed by immunoblotting with antibodies against phosphorylated Threonine, DYNLT1, KIM-1, and GAPDH. The input lane represents 5% of the lysate. The data represents three independent experiments. (b) The ratio of the level of

phosphorylated threonine of same size as DYNLT1 (pThr-DYNLT1) to total DYNLT1 pulled down by IP was determined based on densitometric values obtained from Western blotting ($n = 3$, $^*p < 0.05$, unpaired t-test).

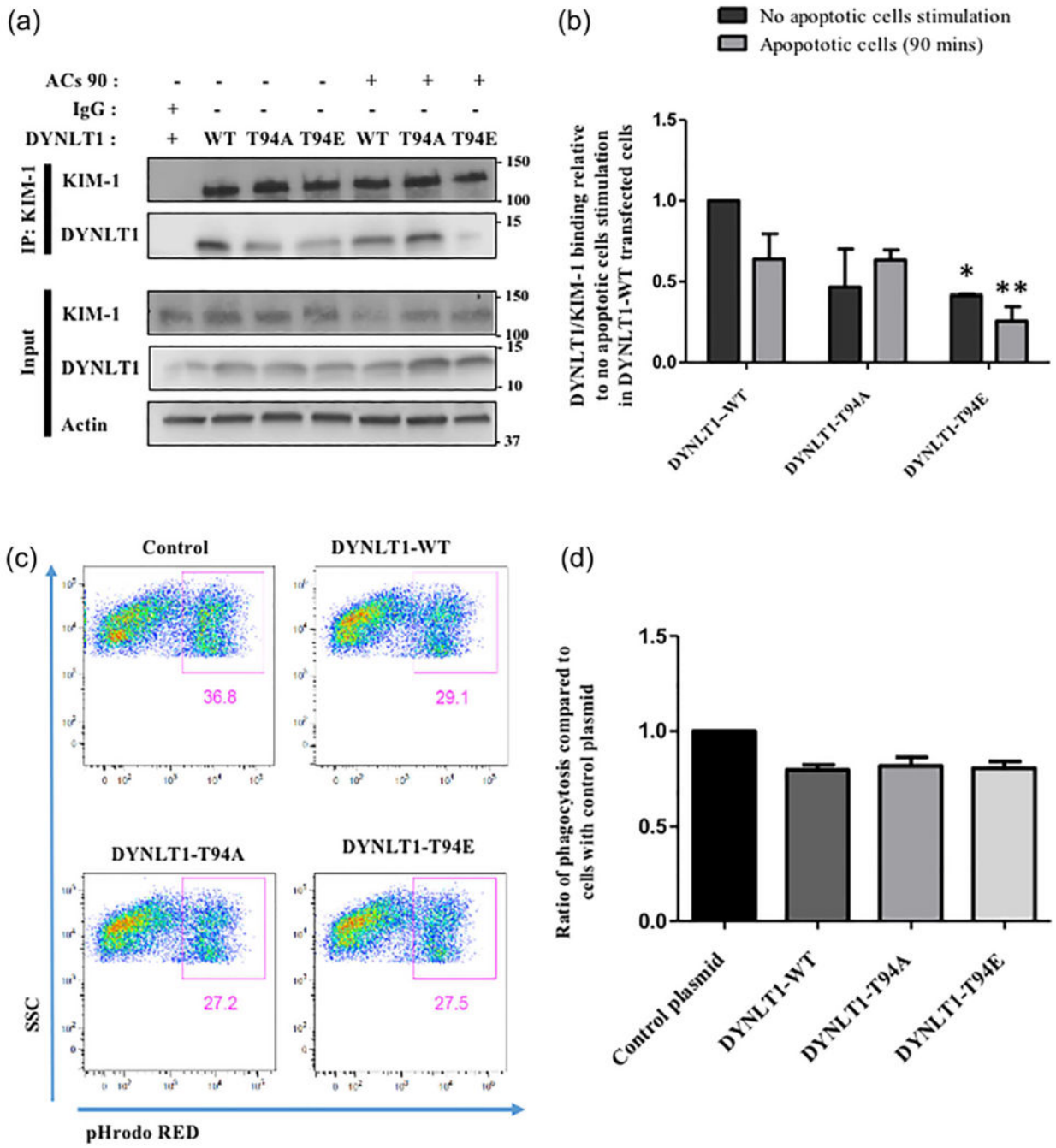

FIGURE 8.

Phosphomimetic mutant of Tctex-1 exhibits a reduced binding to KIM-1, but does not influence KIM-1-mediated efferocytosis. (a) HEK-293 cells were co-transfected with GFP-labeled KIM-1 and either control vector encoding flag-tag, wild type flag-tagged Tctex-1, unphosphorylataed mimic of flag-tagged Tctex-1 (Tctex-1-T94A), or phosphomimetic mutant of flag-tagged Tctex-1 (Tctex-1-T94E). Cells were either unstimulated or stimulated with apoptotic cells for 90 min (ACs 90) and extracts were used for co-immunoprecipitation using KIM-1 antibody as described in the experimental procedures section. All samples

were analyzed by immunoblotting with antibodies against KIM-1, Tctex-1, and actin. The input lane represents 5% of the lysate. (b) The level of Tctex-1 bound to KIM-1 was determined based on densitometric values acquired from Western blotting ($n = 3$, $^{*}p < 0.05$, $^{**}p < 0.01$, unpaired t-test). (c) Cells in (a) were fed apoptotic cells that were fluorescently labeled with pHrodo red for 90 min and the percent of uptake of apoptotic cells was determined by flow cytometry as shown in pHrodo red versus side scatter (SSC) plot. (d) The percentage of phagocytosis was determined based on high pHrodo red fluorescence as measured by flow cytometry ($n = 4$, not significant data, unpaired t-test)

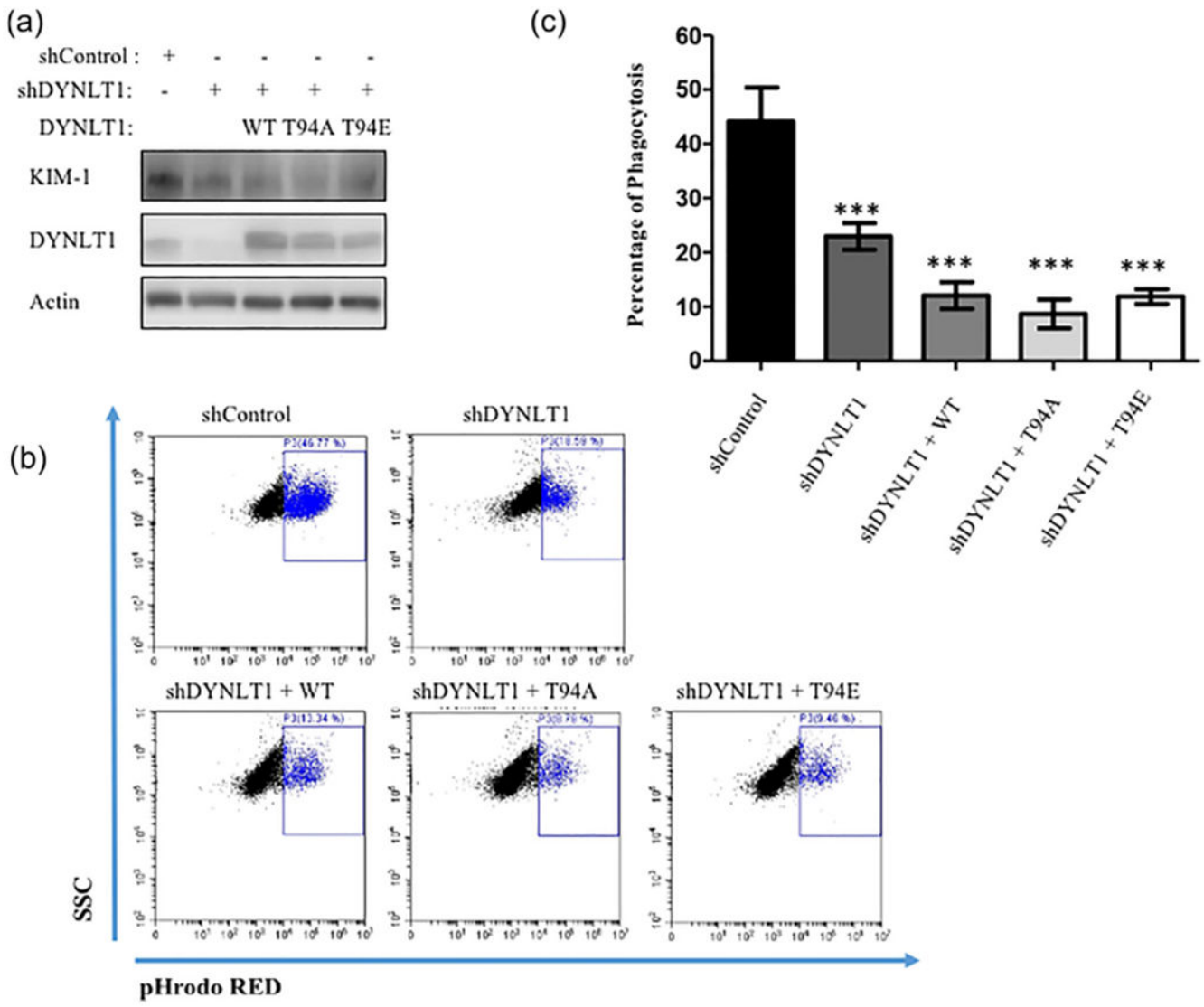

FIGURE 9.

Phosphomimetic mutant of Tctex-1 failed to rescue Tctex-1 function in sh Tctex-1 silenced cells. (a) 769P with Tctex-1 knockdown were transfected with either control vector encoding wild type flag-tagged Tctex-1 (WT), unphosphorylated mimic of flag-tagged Tctex-1 (T94A), or phosphomimetic mutant of flag-tagged Tctex-1 (T94E). Cell lysate were analyzed by immunoblotting to confirm the expression of different forms of Tctex-1 and level of KIM-1 expression. Antibodies against KIM-1, Tctex-1, and actin were used for immunoblotting. (b) Cells in (a) were fed pHrodo red fluorescently-labeled apoptotic cells for 90 min and the percent of uptake of apoptotic cells was determined by flow cytometry as shown in pHrodo red versus side scatter (SSC) plot. (c) The percentage of phagocytosis was determined based on high pHrodo red fluorescence as measured by flow cytometry ($n = 4$, ***$p < 0.001$ compared to shControl and shTCTEX-1 (for WT, T94A, T94E), unpaired t-test). (d) Sh Tctex-1 cells transfected with either wild type flag-tagged Tctex-1 (WT), unphosphorylated mimic of flag-tagged TCTEX-1 (T94A), or phosphomimetic mutant of

flag-tagged Tctex-1 (T94E) were fixed and permeabilized for immunostaining of the Tctex-1 and tubulin. This was done using anti-flag antibody conjugated with AlexaFlour-488 and Cy3 conjugated-anti-tubulin antibodies

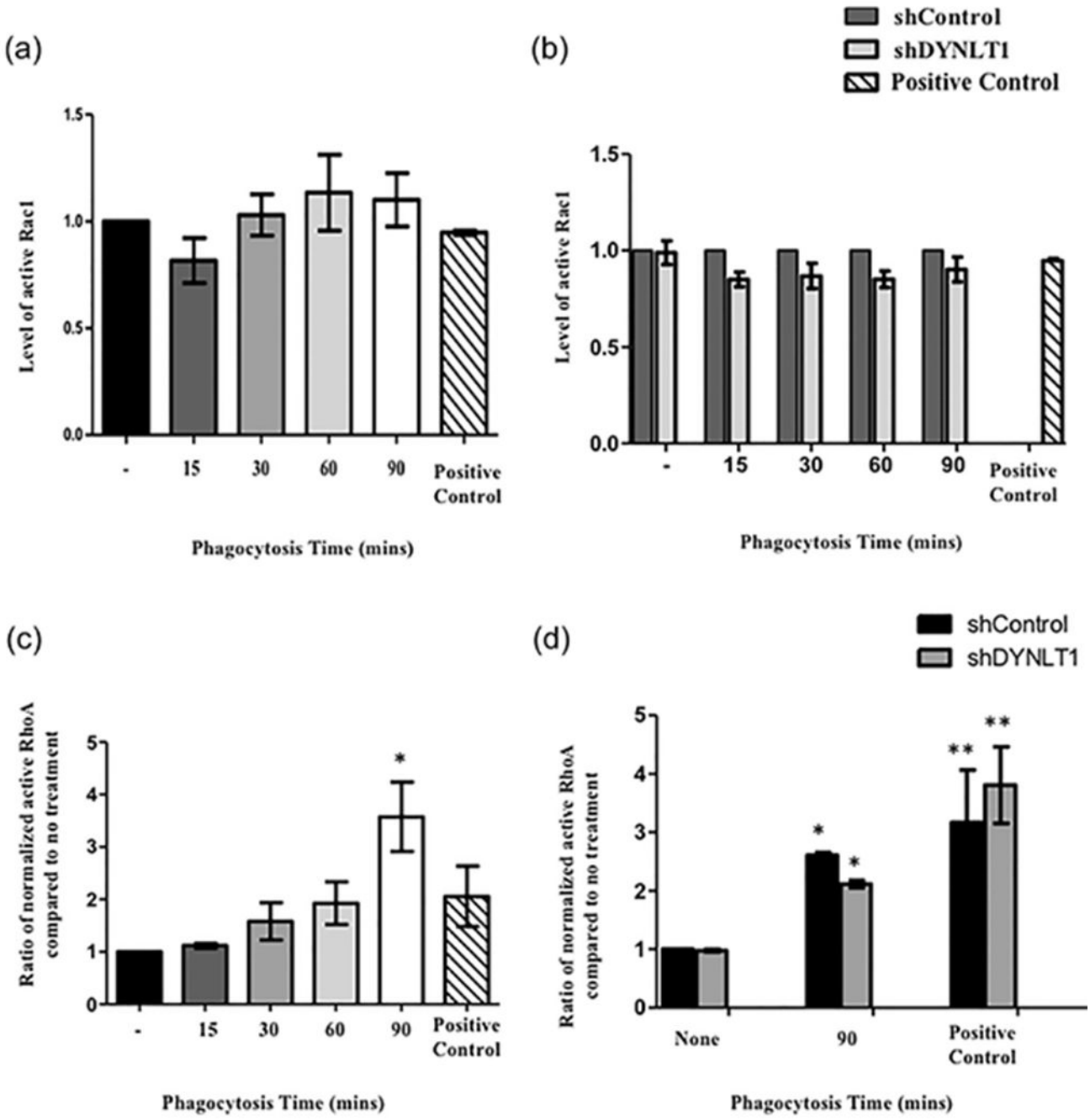

FIGURE 10.

Tctex-1 regulates the actin cytoskeleton independent of RhoA and Rac1 GTPases in KIM-1-mediated phagocytosis. (a) 769-P cells were fed apoptotic cells for various time periods (15–90 min) and the level of Rac1 activation was measured by G-LISA Rac1 activation kit (Cytoskeleton, Denver, CO). ($n = 4$, all not significant, one-way ANOVA). (b) 769-P stably transfected with control (shControl) or shRNA against Tctex-1 (sh Tctex-1) were used. These cells were fed apoptotic cells for various time periods and the level of Rac1 activation was graphed ($n = 5$, all not significant, unpaired t-test). Treatment of 769-P cells transfected

with control siRNA with 5% serum after serum starvation overnight served as a positive control for Rac1 activation (Curtiss et al., 2011). (c) 769-P cells fed apoptotic cells (15–90 min) were subjected to active RhoA and total RhoA assay measurements as determined by the active G-LISA RhoA activation assay and the total RhoA ELISA kit (Cytoskeleton, Denver, CO), respectively. Normalization of active RhoA was done according to manufacturer's recommendation and was graphed to represent data ($n = 3$, all not significant, one-way ANOVA). (d) 769-P cells stably transfected with either control shRNA or TCTEX-1 shRNA were fed apoptotic cells 90 min. The level of normalized active RhoA was determined as in (c) ($n = 4$, $^{*}p < 0.05$, $^{**}p < 0.01$ when compared to shControl no stimulation with apoptotic cells, no significant difference was found between shControl and sh Tctex-1 in all treatments, one-way ANOVA). For positive control for RhoA activation, cells were treated with 10 μM Nocodazole for 15 min (Martin et al., 2001).